ISSN 0020-4412, Instruments and Experimental Techniques, 2018, Vol. 61, No. 2, pp. 239–259. © Pleiades Publishing, Ltd., 2018.
Original Russian Text © K.N. Mitrofanov, V.I. Krauz, E.V. Grabovski, V.V. Myalton, M. Paduch, A.N. Gritsuk, 2018, published in Pribory i Tekhnika Eksperimenta, 2018, No. 2, pp. 78–99.

GENERAL EXPERIMENTAL TECHNIQUES

Features of the Application of the Magnetic-probe Method for Diagnostics of High-temperature Plasma

K. N. Mitrofanov[a,*], V. I. Krauz[b], E. V. Grabovski[a], V. V. Myalton[b], M. Paduch[c], and A. N. Gritsuk[a]

[a] *State Research Center of the Russian Federation, Troitsk Institute for Innovation and Fusion Research, Troitsk, Moscow, 142190 Russia*

[b] *Kurchatov Institute National Research Center, Moscow, 123182 Russia*

[c] *Institute of Plasma Physics and Laser Microfusion, Warsaw, 01-497 Poland*

**e-mail: mitrofan@triniti.ru*

Received March 21, 2017

Abstract—Some aspects of the applicability of the magnetic-probe technique in high-power pulsed discharges are analyzed. The influence of an electron beam and an intense X-ray yield of (~1 TW/cm^2), which result from the compression of high-current plasma in the interelectrode gap of a Z-pinch discharge, on the correctness of measurements using magnetic-field probes was studied. We considered the use of multilayer shells as a method for protecting the sensing element of a magnetic probe. The results of experimental testing of probes of a new design in experiments with wire assemblies on the Angara-5-1 facility at discharge currents of up to 4 MA are presented. Experiments on the Angara-5-1, PF-3, and PF-1000 high-power electrophysical facilities show the effect of the shape and material of the probe shell on the perturbation of plasma that flows around a probe and, as a consequence, on the accuracy of the magnetic-field measurements.

DOI: 10.1134/S0020441218010281

1. INTRODUCTION: MAGNETIC-PROBE MEASUREMENTS IN HIGH-CURRENT DISCHARGES

In physics, there are a number of diagnostic techniques for measuring the magnetic fields in plasma: the methods that are based on the Zeeman effect, magneto-optical Faraday effect, and the magnetic-probe method. The latter method is the most widespread of them; it is the simplest method for measuring the magnetic field at the point of the probe location. Despite this, the use of probes for diagnostics of magnetic fields faces a number of significant difficulties. First of all, this is the difficulty of measuring the magnetic field inside plasma in high-power facilities because of a probable destruction of a probe in a flow of hot particles, the impact of electron beams, which arise in the interelectrode gaps of an installation, and the influence of a high-power X-ray flux on the probe. Because the magnetic-probe method (MPM) is of contact nature, it is necessary to consider both the effects of the probe on the investigated plasma and a possible distortion of the probe signal by surrounding plasma.

Despite the difficulties in using magnetic probes, this diagnostic method was successfully used to measure magnetic fields in fast Z-pinches and plasma-focus (PF) facilities. In a number of works, considerable attention was paid to the analysis of some features of applying the MPM to plasma (for example, the influence of the shape of the probe shell, the plasma flow around the probe shell, the location of loops inside the shell, etc.).

Magnetic probes for measuring the magnetic fields in the vicinity of the insulator of a Mather-type PF installation were used in [1]. Measurements were performed in the gaseous deuterium medium at an initial pressure of 0.5–5 Torr and an energy of ~4.7 kJ stored in the battery. The probe signals were calibrated against a signal from a Rogowski coil for different positions of the magnetic probe, when the installation operated in the short-circuit mode. However, the calibration of probes against a signal from a Rogowski coil as a standard current sensor showed the double excess of the probe-measured current over the total current of the installation during an experiment on the current-plasma sheath (PCS) compression.

It is quite possible that in this case, the overestimation of the probe-measured current occurred due to a strong perturbation of the plasma sheath by the probe shell. In [1], the probe signals were expressed in the

units of the probe voltage (in volts) and the magnetic-field value could not be evaluated. However, the time characteristics of signals, namely, the time of occurrence and the time profile of probe signals, made it possible to determine the spatial and dynamic characteristics of the plasma sheath. Important information on the initial stage of the PCS evolution in the region of the insulator of the PF installation was obtained from measurements that were performed using magnetic probes. Probe signals were used to evaluate the radial current distribution inside the PCS. The radial velocity of the PCS motion at the final compression stage was determined: $V_r \approx (2.5–3.5) \times 10^6$ cm/s. It was shown for the entire accessible range of the initial gas pressures that the PCS is inside the volume between the anode electrode and pin cathode electrodes and that the PCS thickness is smaller near the insulator than at large radii.

The current distribution at the PCS acceleration stage was investigated in [2]. Azimuthal magnetic fields were investigated in the accelerating part of a Mather-type PF facility. In this case, the probes were positioned along the entire length of the accelerating part of the facility. The experiments were conducted with nitrogen at a pressure of up to 10 Torr and a storage energy of ~15.4 kJ. In this paper, we also consider the problem of the influence of the electrode material on the current flow in the PCS. The probe measurements of the magnetic fields in the accelerating part of the installation and the snowplow model were used to show that the plasma mass of the PCS, which gathers the gas during its compression, contains a certain additional mass of the electrode substance.

In order to correctly measure the magnetic field in a dynamic plasma stream with a frozen magnetic field, some processes must be taken into account: the plasma flow around the probe shell and the plasma formation at the probe surface under the action of a radiation flux from plasma on the probe. The qualitative understanding of these physical processes requires investigations of the plasma behavior near the probe: the flow-around velocity, the time of the magnetic-field diffusion from plasma inside the probe shell, the degree of perturbation of the plasma stream by the probe, and the determination of the plasma density and temperature around the probe.

One of the attempts to analyze the effects of the plasma flow around the probe, its interaction with the probe shell, and the influence of these effects on the probe-measured magnetic field was made in [3]. The dependence of the measured magnetic-field value on both the location point of the measuring loops inside the probe shell and the thickness of the current sheath that flows around the probe was investigated in this study. The analysis was performed on the basis of the solution of a stationary problem under the assumption that the PCS plasma that hits the probe has a constant velocity. It was shown that the shape of the probe shell may have a significant effect on the value of the probe-measured magnetic field. Note that the magnetic-field diffusion from hot plasma into the probe shell was disregarded in [3] when analyzing the influence of the process of the plasma flow around the probe shell.

As a rule, in such experiments, a probe interacts with a supersonic magnetized-plasma flow that moves at the velocity $V_r > V_A$, where V_A is the Alfven velocity. In [4, 5], the flow of the plasma stream with a frozen-in magnetic field around the probe shell and its influence on the probe-measured magnetic-field value were considered in two approximations: analytically for the subsonic flow-around and numerically for the supersonic flow-around. These papers described the probe technique for measuring the magnetic field inside the plasma of a current-compressed liner on the Angara-5-1 facilities [6]. Measurements were performed at a current in a load of up to 4 MA and a soft X-ray (SXR) power flux to the probe surface of up to 1 TW/cm^2.

The performed analytical and numerical calculations show the importance of the choice of the probe-shell shape. It was shown that the choice of a flat shell of the probe with a size that is smaller than the plasma skin-layer thickness should be preferred in order to reduce the shell cross section for the incoming plasma stream and, consequently, reduce the plasma perturbation. The calculated degree of perturbation of the magnetic field (B_{meas}/B_0), which is introduced by a cylindrical probe, was as high as ~60%; for a flat probe, it was 7%. Calculations of the time of the magnetic-field diffusion into the flat-probe shell yield ≈1.5 ns, which determines the time resolution of the MPM.

One specific feature of using the MPM technique under the conditions of the Angara-5-1 facilities is associated with the fact that the probes are subjected to high-power plasma streams and X-ray fluxes, which lead to probe destruction. In principle, the characteristics (sensitivity, time resolution) of the probes may vary even before their physical damage as a result of the probe-substance ablation and the plasma formation on the probe surface. Estimates and experiments showed that plasma that arises at the probe surface has insufficient time to be heated to a temperature of higher than several electronvolts and, hence, does not lead to appreciable magnetic-field shielding [4].

The magnetic-field freezing-in into the liner plasma is also an important factor in measurements. This field must have enough time to diffuse from the plasma that flows around the probe inside the probe shell, where the measuring loops are located. To reduce the measurement error that is related to the magnetic-field freezing-in into plasma, the probe size must not exceed the plasma skin-layer thickness [7]. In experiments on the Angara-5-1 facilities and PF-3 and PF-1000 plasma-focus facilities, it was shown that perturbations that are introduced by probes into

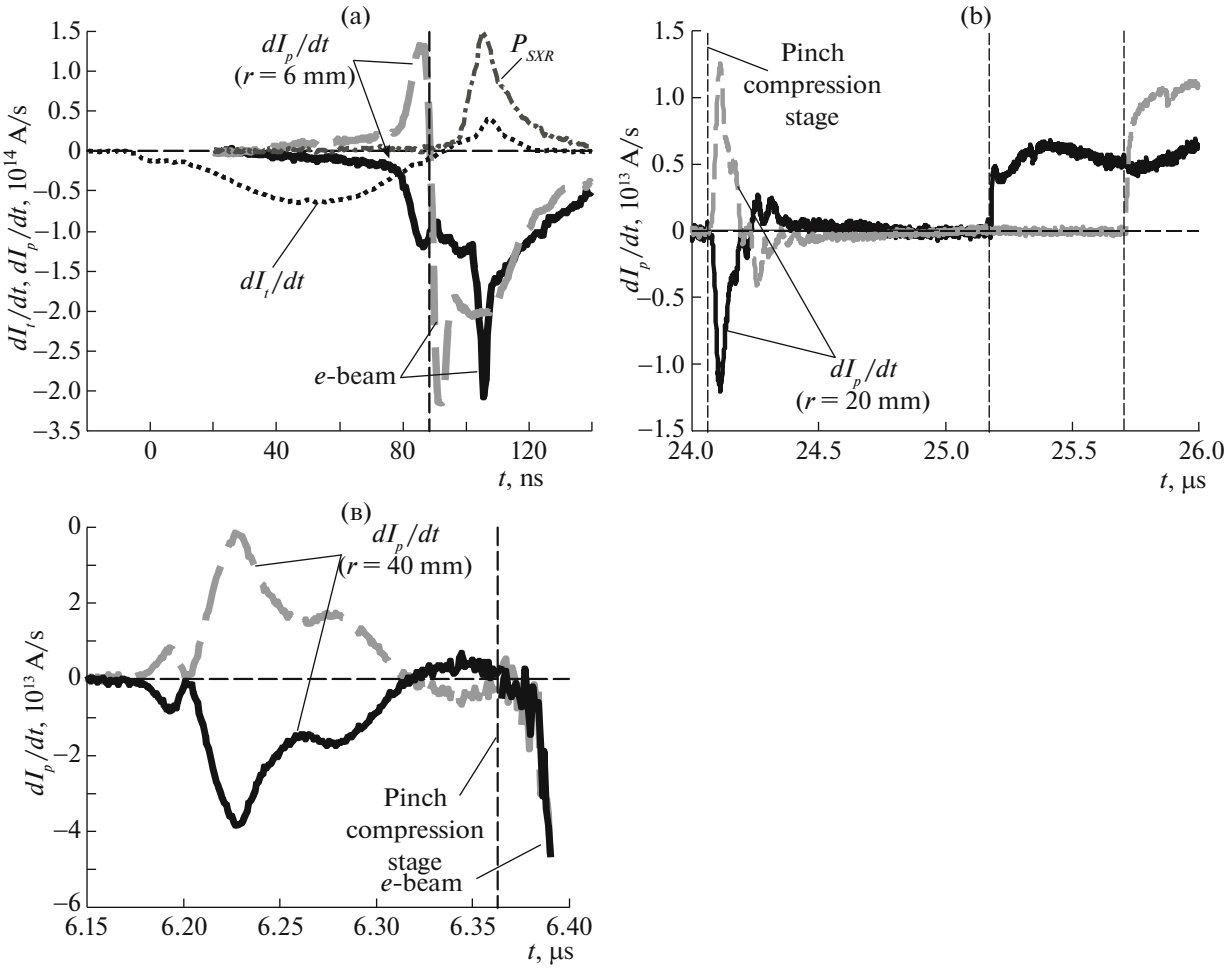

Fig. 1. The typical time dependences of the total-current derivative dI_t/dt and the signal from the magnetic probe, which is converted into the current derivative dI_p/dt, an X-ray power pulse P_{SXR} (in rel. units) for the facilities: (a) Angara-5-1 (the probe has the anode potential), shot no. 4786; (b) PF-3 (the probe has the cathode potential), shot no. 4029; and (c) PF-1000 (the probe has the anode potential), shot no. 8220. Vertical dashed lines mark the time at which the probe stops to reliably operate.

plasma do not lead to a significant change in the discharge conditions: the characteristics of X-ray and neutron radiations and the pinch parameters remain virtually constant.

Paper [8] presented the results of studies of low-energy plasma in the accelerating part of the PF installation. For this purpose, a small high-frequency magnetic probe with a response time of ~1 ns was designed. The probe consisted of two coils with a diameter of ~0.7 mm. In the opinion of the authors, such a probe was unable to perturb the plasma stream, although this was not analyzed in their study. The magnetic probe was calibrated in the magnetic field of the Helmholtz coil, thus providing a high calibration accuracy (up to ~5%). The sensitivity and frequency characteristic of the probe sensor were optimized (as was done in [9]). The measurements were performed in the nitrogen medium at a pressure of ~0.3 Torr with an energy of ~2.2 kJ in the battery. As a result of magnetic-field measurements, the average current thickness of the sheath was evaluated as 3 cm at the stage of the shell motion in the accelerating part of the installation electrode system. The "lost" current and mass behind the PCS were ~32 and ~40%, respectively.

The PCS dynamics in the region of the insulator of the installation and the arrival of plasma at the anode edge were investigated using the MPM on the Sahand installation (Iran, Filippov-type PF) [10]. It should be noted that the probes were not calibrated in [10] and only the time characteristics of their signals were used. These experiments were performed with neon in a range of the initial pressures of 0.25–1 Torr and a stored energy of 14–50 kJ.

The radial and axial components of the PCS motion velocity were determined from the magnetic-probe measurements: $V_r \approx (4 \pm 0.13) \times 10^6$ cm/s and $V_z \approx (3.51 \pm 0.22) \times 10^6$ cm/s. The authors stated that the radial velocity of the PCS motion was slightly

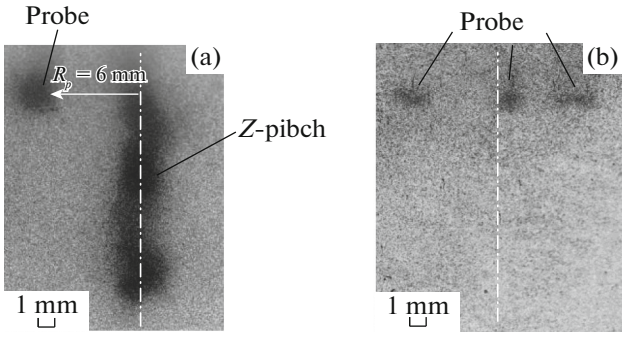

Fig. 2. The glow of the probe shell. Images that were obtained with an integral pinhole camera for photons with energies $h\nu > 20$ keV upon shrinkage of the Z-pinch of wire assemblies on the Angara-5-1 facility (the anode is at the top, the cathode is at the bottom): (a) shot no. 4669, experiment with one probe inside a tungsten wire array; and (b) shot no. 5012, experiment with three probes inside an aluminum wire array.

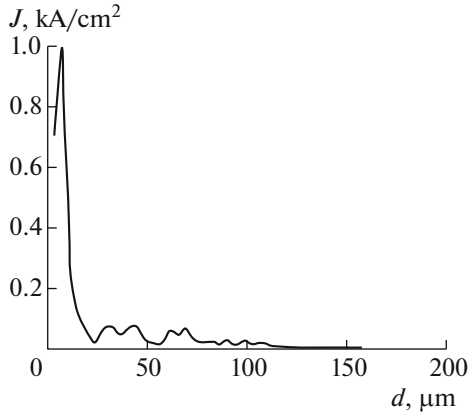

Fig. 3. The calculated current-density distribution in the foil thickness for an electron beam that penetrated into the NbTi-foil material of the probe shell.

higher than the PCS axial motion. In addition, the influence of the charging-voltage level of the battery (10–18 kV) on the PCS dynamics, namely, on its motion velocity, was also considered in [10].

The influence of the presence of a magnetic probe on the PCS dynamics near the focus and on the discharge as a whole was studied in [11]. Experiments were performed with argon in a range of the initial pressures of 0.25–3.25 Torr at a stored energy in the battery of the installation of ~3.6 kJ (the PF of the Mather type). The main results of this study were as follows. In the presence of a probe, several focus-compression regions are formed, plasma is attached to the probe, and the electron emission and X-ray radiation that accompanies it are intensified. It should be noted that in these experiments, the probe was rather large (~6 mm in diameter), and this could have a negative effect on the discharge as a whole.

In [12], a Filippov-type PF facility at a deuterium pressure of ~0.2 Torr and an energy of ~60 kJ in the battery was used to investigate the radial stage of the PCS compression in the region of the facility. It was shown that several plasma sheaths may be formed, thus negatively affecting the neutron yield. In this case, the probe registers an incomplete discharge current (~50% of the total current). "Eddy" toroidal currents were discovered in the residual plasma that surrounded the pinch. Note that in order to determine the time of the formation of closed current loops (which may be formed in the residual plasma behind the PCS) and the number of loops more accurately, it is necessary to use a larger number of probes and place them at different radii from the installation axis.

The results of the experiments that were performed on the Puma PF-type facility ($C = 0.75$ mF, $U = 100$ kV, and the maximum stored energy was ~3.75 MJ) with combined pulsed gas puffing (deuterium up to 10 Torr) and a current rise time of 6 μs to a maximum current of 3 MA were presented in [13]. The experiments were performed at an energy in the capacitive storage unit of ~0.93 MJ. The electric-current distribution over the gap was investigated using magnetic probes, which were located at the most typical points: near the insulator, near the turn of the current layer at the anode edge, and at a distance of 15 cm from the axis of the facility. All the probes were calibrated against the total current. The probes were not installed very near the facility axis. The measurements that were performed using magnetic probes have shown that for high neutron yields (up to 5×10^{11} neutrons/pulse), the entire current outgoes into the region with a radius of 15 cm.

Thus, it can be stated that the most substantial factors that restrict the use of magnetic probes in high-power discharges are as follows: the evaporation of the probe shell under the action of X-rays and corpuscular flows, plasma shielding of magnetic probes, the plasma perturbation during its flow around the probe shell, and the impact of electron beams that arise in the interelectrode gap of the facility on the probe.

The objective of this study was:

(i) to investigate the influence of an electron beam, which is generated in the interelectrode gap at the final plasma-compression stage, and the intense X-ray yield (up to 3 TW, $h\nu > 100$ eV) on the registration of the magnetic field by probes;

(ii) to develop variants of the magnetic-probe design with protection against the influence of the electron beam; to choose the shape and material of the probe shell for its improved flow-around by plasma;

(iii) to extend the time of reliable magnetic-field registration by a probe in plasma;

(iv) to experimentally test the working capacity of the newly designed probes.

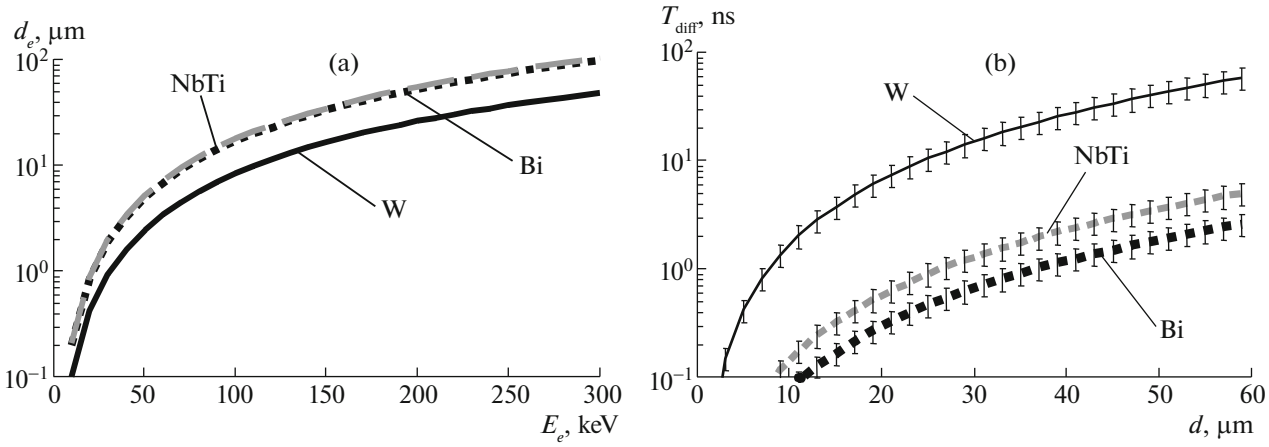

Fig. 4. The calculated dependences: (a) electron penetration depths into various substances of the probe shell as functions of their energy according to (2); (b) the time of the magnetic-field diffusion into the probe-shell substance as a function of the shell thickness according to expressions (3). The estimates according to the expressions for T_{diff}^{garm} and T_{diff}^{step} are shown in the curves as the time spread.

2. THE DURATION OF THE MAGNETIC-FIELD REGISTRATION IN PLASMA. PROBES WITH MULTILAYER SHELLS

First, let us consider some experimental facts that helped us to determine the reason that a magnetic probe had a limited time of operation inside plasma, which was formed by a multiwire array on the Angara-5-1 installation at the TRINITI State Research Center of the Russian Federation and deuterium pinches in the PF-3 and PF-1000 plasma-focus facilities at the Kurchatov Institute National Research Center and the Institute of Plasma Physics and Laser Microfusion (IPPLM, Poland), respectively.

The design of the sensing element of the magnetic probe consisted of two separate loops with diameters of 300–800 μm that were wound clockwise and counterclockwise [4, 5]. This design of the probes provided bipolar signals fed to oscilloscopes in the magnetic-field measurements. The criterion for a disturbance in the sensor operation was a similarity violation with consideration for the bipolar nature of the recorded signals. The signal from each loop of the probe was proportional to the magnetic-field derivative ($U_p \propto \partial B/\partial t$) at the point of the probe location.

The current that flowed inside the radius of the probe position relative to the installation axis was calculated via the numerical integration of the measured curve $\partial B/\partial t$ taking the obtained calibration coefficients into account and assuming that the current plasma is symmetric relative to the facility axis: $I = K\int(\partial B/\partial t)dt$. The calibration coefficients K were obtained when testing the serviceability of probes in a pulsed magnetic field of a Helmholtz coil, as was described in detail in [4, 5].

Figure 1 shows typical probe-signal oscillograms from [5, 14–18] that were obtained in experiments on the above facilities. In all cases, the probe was located near the axis of the facility (0.6–4 cm from it).

It follows from the probe oscillograms that under conditions of experiments on the Angara-5-1 facility the operating interval of time of the MPM technique lasts ~90 ± 10 ns. Under the conditions of experiments on the PF facilities, the measurement time is up to 1 μs for the PF-3 and 200–300 ns for the PF-1000.

Note that in these facilities, the magnetic probe could be introduced into the discharge chamber from both the anode side (Angara-5-1 and PF-1000) and from the cathode side (PF-3). As follows from experiments, at the time when the operation of magnetic sensors is disturbed, unipolar signals usually begin to be registered, which are not associated with changes in the magnetic field at the probe location point. In the cases where the probe had the potential of the anode electrode, after this time, signals of negative polarity were recorded. When the probe was at the cathode potential, signals of positive polarity were recorded.

Most likely, the probe that is at the anode potential is affected by the electron beam. When the electron flow arrives at the wire of which the probe loops are made, it partially transfers its charge to the wire. In this case, the probe starts to register the electron-beam charge and signals become negative. This fact can be confirmed by the time-integral pinhole patterns of the probe-shell glow in the spectral range of photon energies $h\nu > 20$ keV (see Fig. 2), which is initiated under the impact of the electron beam [19]. The figure shows that the end of the probe shell facing the cathode generally glows. Electrons with a certain energy penetrate inside the probe shell. The experimental and theoreti-

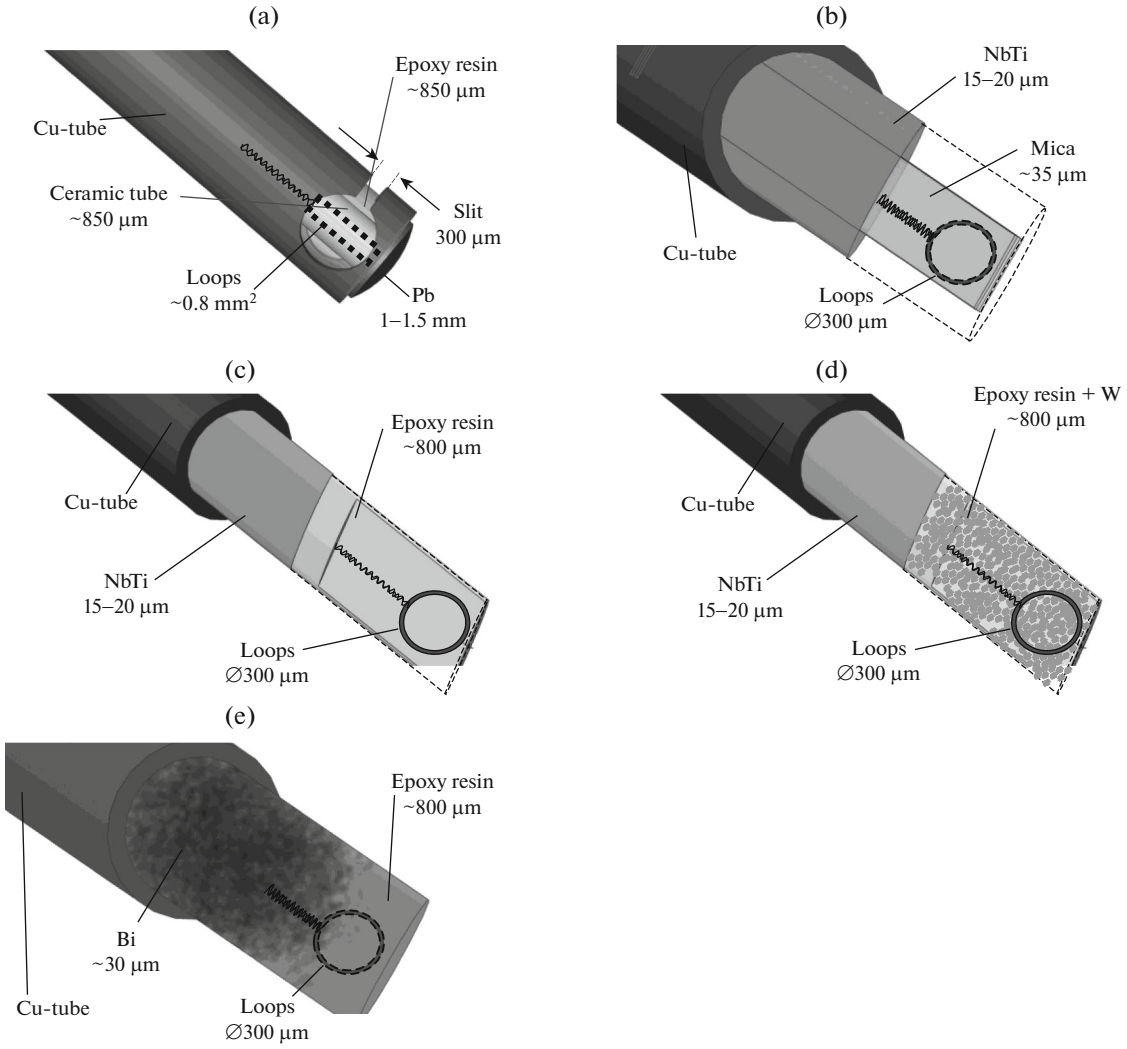

Fig. 5. The structures of the sensitive elements of probes with cuts along the layers of the protection shell: (a) a cylindrical probe in a copper tube with a 300-μm slit for a magnetic field, the tube end is closed with a lead plug against a *e*-beam; (b) a probe with a flat mica shell coated with a 15–20-μm-thick NbTi foil; (c) a probe with a flat epoxy-resin shell coated with a 15–20-μm-thick NbTi foil; (d) a probe with a flat shell of epoxy resin doped with a W powder (50% resin, 50% W) and coated with a 15–20-μm-thick NbTi foil; and (e) a probe with a flat epoxy-resin shell with an evaporated ~30-μm-thick bismuth coating.

cal estimates of the energy of such electrons will be given below.

In the case where the probe is at the cathode potential and located near the axis of the installation ($r <$ 2 cm on PF-3), the plasma potential is applied to the probe loops after the plasma pinching stage and the correct operation of the magnetic probe is disturbed. In this case, positive signals are recorded (Fig. 1b).

It is known that in experiments with pinches, a high voltage [15, 20] and electron leakage [21, 22] arise during the final plasma compression in the electrode gap of the facility. It follows from the experiments on measuring the electron-beam current that were carried out on the Angara-5-1 installation [22] that an electron beam with the electron energy $E_e > 200$ keV arises 5–10 ns after the peak of SXR radiation (soft X rays, $h\nu > 100$ eV). Its duration is ~20–50 ns. The lower estimate of the beam-current density was $J \approx 70$ kA/cm^2.

At the same time, an electron beam with energies of 50 keV $< E_e <$ 200 keV arises 20 ns before the occurrence of the SXR peak [21]. The beam duration was approximately 20–30 ns. The maximum measured current density of the electron beam was $J_{max} \approx 1.5$ kA/cm^2. The parameters of this beam will be taken as the upper estimate of the electron-beam absorption in the material of the probe shell before the time of the SXR peak.

The range of electrons R_x [g/cm^2] of these energies ($0.01 \le E_e \le 3$ MeV) in the probe-shell material (NbTi foil) was calculated according to [23] in the following manner:

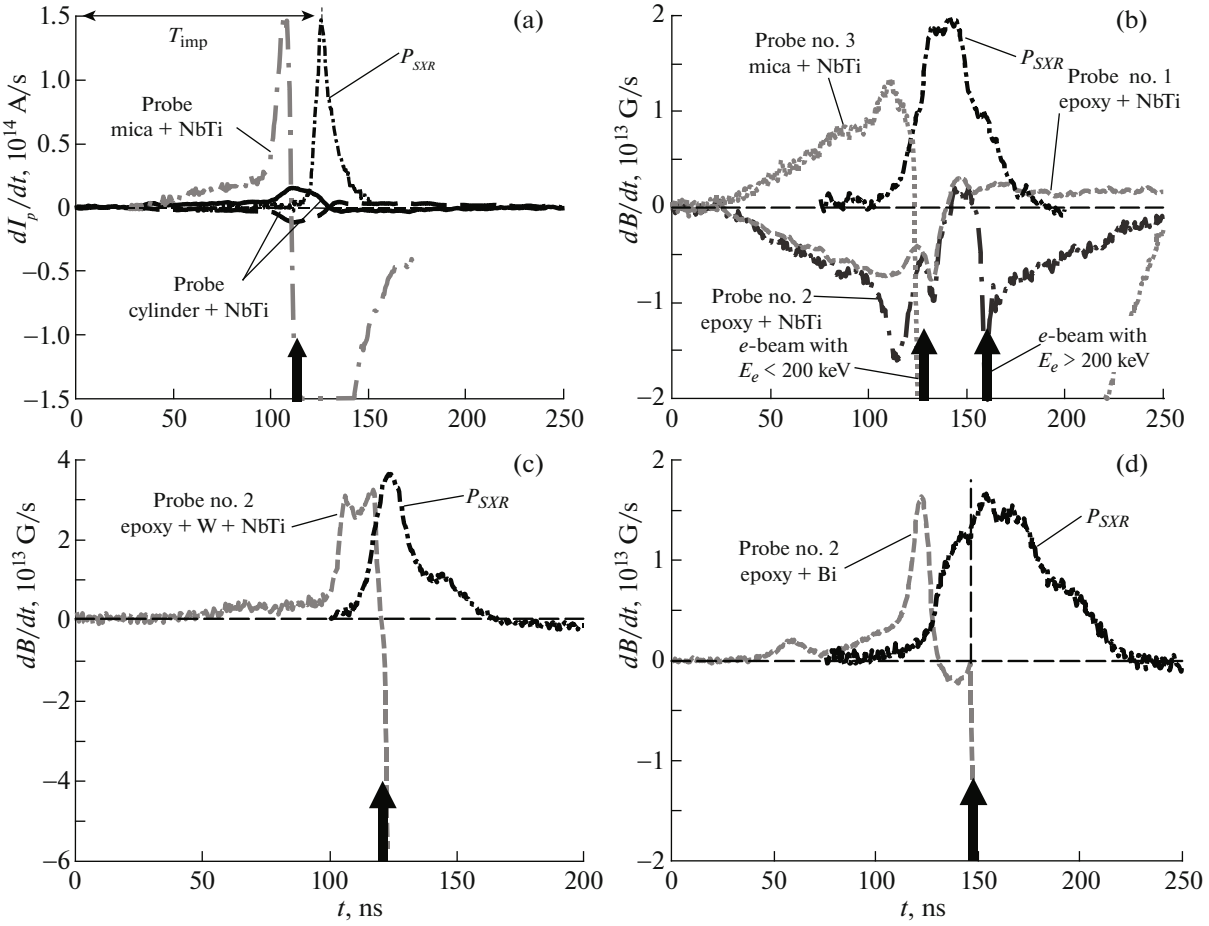

Fig. 6. The results of recording magnetic fields inside plasma of the wire array on the Angara-5-1 facility. An error marks the time of the start of the electron-beam action on the probe. P_{SXR} is the SXR power pulse (in arb. units), T_{imp} is the implosion time of the wire array. Shots: (a) no. 3648, no. 4786: a probe (cylinder + NbTi) with a cylindrical copper shell (∅3 mm) with a slit for a magnetic field, which is covered by a NbTi foil with a thickness of 15–20 μm, a probe (mica + NbTi) with a flat mica shell, which is covered by a NbTi foil with a thickness of 15–20 μm, the probes are positioned at a radius of 5 mm; (b) no 4880: probes nos. 1 and 2 with a flat epoxy-resin shell covered with a 15–20-μm-thick NbTi-foil shield, probe no. 3 with a flat mica shell covered with a 15–20-μm-thick NbTi foil, the probes are positioned at a radius of 8.5 mm; (c) no. 4923: probe with a flat shell of epoxy resin doped with a W powder (50% resin, 50% W) and coated with a 15–20-μm-thick NbTi foil; and (d) no. 5092: probe with a flat epoxy-resin shell with an evaporated 31-μm-thick bismuth coating, which is positioned at a radius of 5 mm.

$$R_x(E_e) = R_{\mathrm{Al}}(E_e)\frac{(Z/A)_{\mathrm{Al}}}{(Z/A)_x}, \qquad (1)$$

where $R_{\mathrm{Al}}(E_e) = 0.412E_e^n$, $n = 1.265–0.0954\ln E_e$ is the range of electrons with the energy E_e [MeV] in aluminum, and Z/A is the ratio of the element charge to its atomic mass. For the NbTi alloy, $Z/A \approx 0.565$; according to formula (1), the range of electrons then was $R_x \approx$ 4.3 mg/cm^2 (for electrons with $E_e = 50$ keV), which is smaller than the surface density of this material 6.54–9.81 mg/cm^2 at a thickness of the NbTi foil of 10–15 μm. Hence, it follows that electrons with energies $E_e \le 50$ keV are completely absorbed in the material of the probe shell.

Along with this estimate, we performed a numerical simulation of the penetration of a monoenergetic electron beam ($E_e = 150$ keV, the duration $\Delta t = 50$ ns) with a beam-current density of 1 kA/cm^2 into the probe-shell material, NbTi foil. The calculation was made within the framework of the radiation magnetohydrodynamic model of a supersonic plasma flow around the probe shell [5]. Figure 3 shows the calculated current-density distribution of fast electrons that penetrated inside the probe shield over the thickness of the probe shell $J(d)$. As is seen in Fig. 3, electrons are mainly absorbed at a depth of 10–20 μm, but their small part (1–3%) propagate to a depth of up to 150 μm. This causes the incorrect operation of magnetic probes at the instant of plasma pinching.

Figure 4a shows the results of calculating the penetration depth of electrons d_e of various energies into some probe-shell materials, that is, NbTi, tungsten, and bismuth, using the following expression:

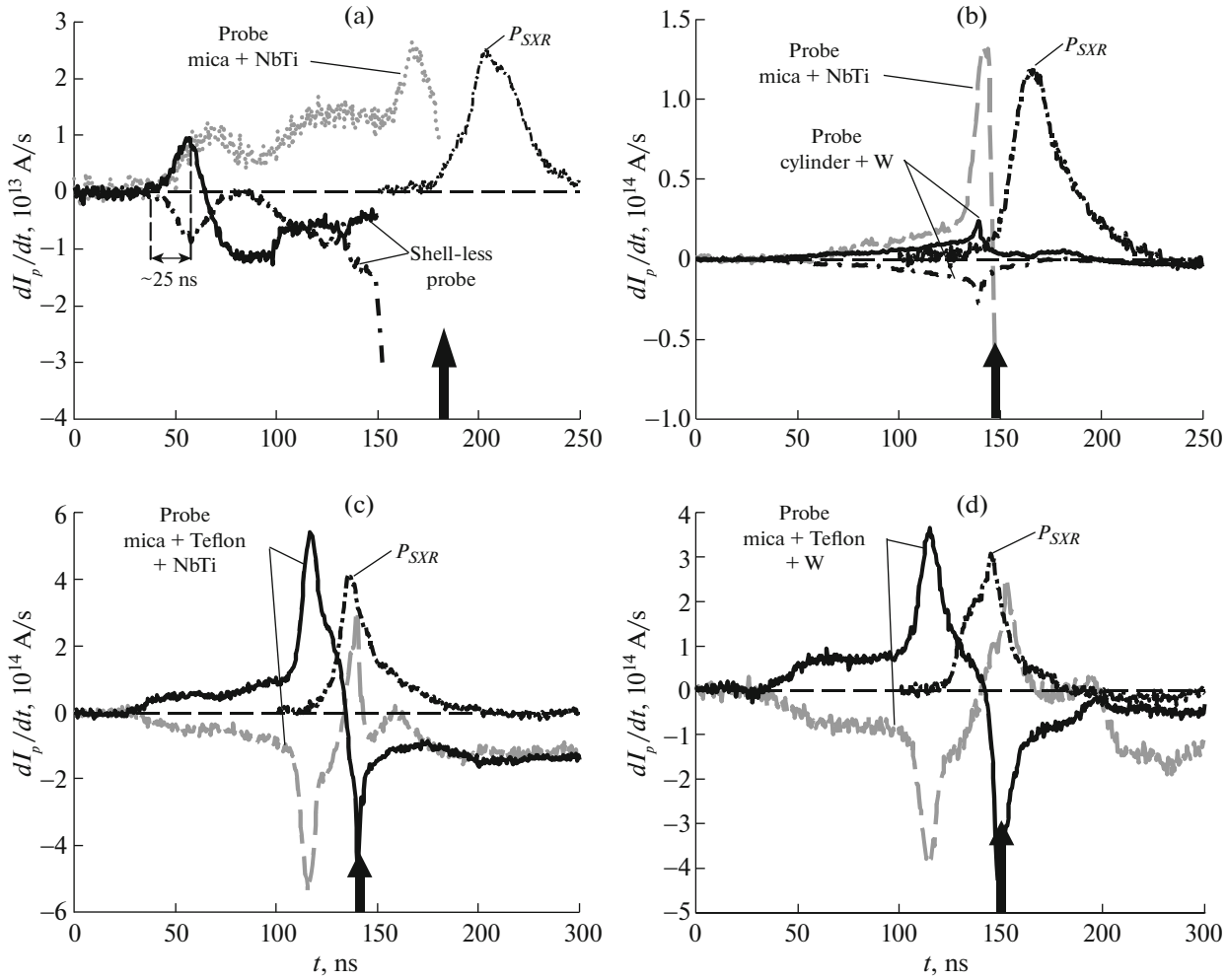

Fig. 7. The results of recording the magnetic fields inside plasma of a wire array on the Angara-5-1 facility. An error marks the time of the start of the electron-beam action on the probe. P_{SXR} is the SXR power pulse (in arb. units). Shots: (a) no. 3960: a probe with open loops (without a shell), a probe (mica + NbTi) with a flat mica shell, which is covered with a 15–20-μm-thick NbTi foil; the probes are positioned at a radius of 7.5 mm; (b) no. 3889: a probe (cylinder + W) with a cylindrical shell (∅1.2 mm), which is covered with a 20-μm-thick W foil, a probe (mica + NbTi) with a flat mica shell, which is covered with a 15–20-μm-thick NbTi foil, the probes are positioned at a radius of 5 mm; (c) no. 3899: a probe (mica + Teflon + NbTi) with a flat mica shell, which is covered with a 20-μm-thick Teflon film and a 15–20-μm-thick NbTi foil, the probe is positioned at a radius of 5 mm; and (d) no. 3895: the probe (mica + Teflon + W) with a flat mica shell, which is covered with a 20-μm-thick Teflon film and a 20-μm-thick W foil, the probe is positioned at a radius of 5 mm.

$$d_e(E_e) = R_x(E_e)/\rho, \quad (2)$$

where $d_e(E_e)$ [cm] is the depth to which an electron with the energy E_e penetrates until it is completely absorbed by the probe-shell substance with the density ρ [g/cm^3].

It follows from Fig. 4a that for shells made of NbTi and bismuth almost the same electron-absorption efficiency is observed. When the shell thickness exceeds 20 μm, the full absorption of electrons with energies below 100 keV will be observed. A somewhat smaller shell thickness (8–9 μm) is needed for tungsten to completely absorb electrons with such energies.

As was mentioned above, in experiments on the compression of the Z-pinch of wire assemblies, high-energy electrons (E_e > 100–200 keV) are registered at the final implosion stage, viz., at the instant of the pinch formation and slightly later. In order to reliably protect magnetic sensors against electrons of such energies, thicker shells must be used. For NbTi (or Bi), it is necessary to use shells with thicknesses d > 20 μm, while for tungsten, $d \geq 10$ μm. On the one hand, tungsten shells are advantageous with respect to NbTi or Bi shells in the electron-absorption efficiency, but they are inferior in the time of the magnetic-field diffusion through the shell material (see Fig. 4b). This considerably impairs the temporal resolution of the magnetic-probe diagnostics. The time of the magnetic-field diffusion through the thickness of the conducting probe

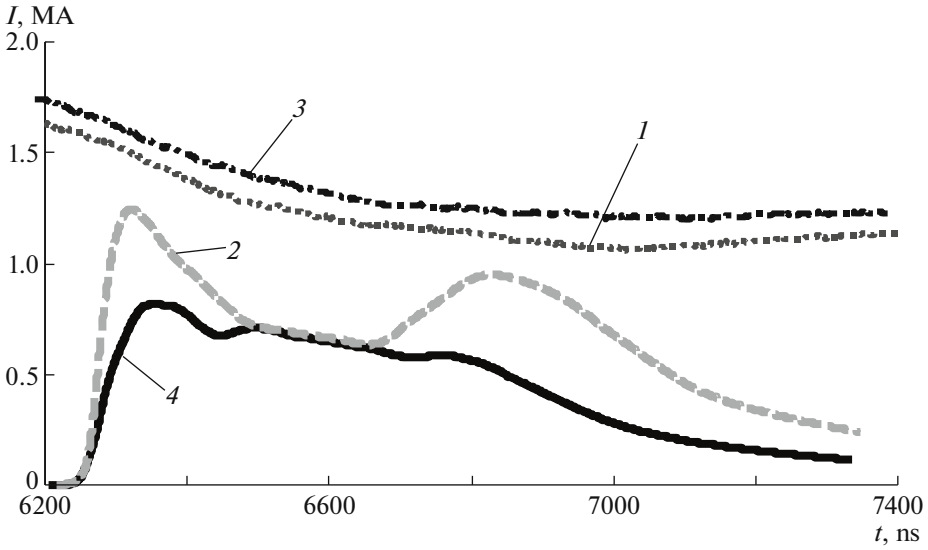

Fig. 8. The comparison of the results of measuring the current in the paraxial region of the PF-1000 facility ($r = 40$ mm) using magnetic probes with different shell shapes. Gaseous D_2, $P_0 = 1.8$ Torr, $U_0 = 24$ kV, $W_0 = 384$ kJ: (*1*, *2*) the total current and the current measured with a probe with a flat shell (mica + NbTi), respectively, in shot no. 9341 ($Y_n = 6.9 \times 10^{10}$ neutrons/pulse); (*3*, *4*) the total current and the current measured with a cylindrical probe (ceramic tube with 2.5 mm in diameter) in shot no. 9340 ($Y_n = 9.8 \times 10^{10}$ neutrons/pulse).

shell was assessed under two assumptions: harmonic oscillations of the magnetic field ($T_{\text{diff}}^{\text{garm}}$) and a response to a magnetic-field pulse in the form of a step ($T_{\text{diff}}^{\text{step}}$), according to the expressions

$$T_{\text{diff}}^{\text{garm}}, \quad s = 10^{-6} d^2/\rho_\Omega,$$
$$T_{\text{diff}}^{\text{step}}, \quad s = 2\pi 10^{-7} d^2/\rho_\Omega, \qquad (3)$$
$$T_{\text{diff}}, \quad s = 0.5(T_{\text{diff}}^{\text{garm}} + T_{\text{diff}}^{\text{step}}),$$

where d, m, is the thickness of the conducting probe shell with the resistivity ρ_Ω [Ω m]. Note that the time estimates $T_{\text{diff}}^{\text{garm}}$ and $T_{\text{diff}}^{\text{step}}$ differ from one another by a factor of at most 1.6, which does not exceed the accuracy of our estimate. Subsequently, the obtained estimates of the times were averaged (the time T_{diff}). Thus, for a tungsten shell thickness of 10–20 μm, the time T_{diff} ranges from 1.5 to 8 ns. For NbTi or Bi shells, this time is appreciably shorter than 0.6 ns. Even for a Bi shell with a thickness of up to 40 μm, this time is no longer than 1 ns.

Based on the calculation results that are presented in Fig. 4, magnetic probes with multilayer shells for shielding the electron beam were constructed. Multilayer flat shells of probes could consist of mica (or epoxy resin) coated with a thin NbTi foil with a thickness of 15–20 μm with (or) an additionally deposited ~31-μm-thick bismuth layer. The design and parameters of the probes with multilayer shells are shown in Fig. 5. In some cases, in the epoxy resin that contained loops, additives of fine-dispersed tungsten powder with an effective diameter of grains of 3 to 15 μm were present. Such multilayer shells reliably shielded the probe loops against an electron beam with an energy of at most 150 keV.

3. EXPERIMENTAL TESTING OF THE DURATION OF THE CORRECT MAGNETIC-FIELD REGISTRATION BY PROBES

At the stage of the refinement of the magnetic-probe diagnostics on the Angara-5-1 installation in the experiments on measurements of the magnetic field plasma with a high energy release, probes with cylindrical copper shells that were thicker than the skin layer of the magnetic field in plasma were used. A slit with a width of ~300 μm for the magnetic-field penetration was cut in the copper shell of the probe with a 3-mm diameter, as shown in Fig. 5a. The magnetic probe consisted of two miniature loops that were wound in different directions (clockwise and counterclockwise). The area of the loops was ~0.8 mm^2 (for 1 turn). The measuring loops were created in a ceramic cylindrical frame. In order to avoid short-circuiting and filling of the slit with plasma, the slit was covered with a 0.02-mm-thick Teflon film with an NbTi foil shield (15–20 μm). The end of the cylindrical copper screen was closed with a lead plug in order to avoid an influence of the electron beam on the probe.

Experiments with this type of probe demonstrated that this design is stable under the action of electron

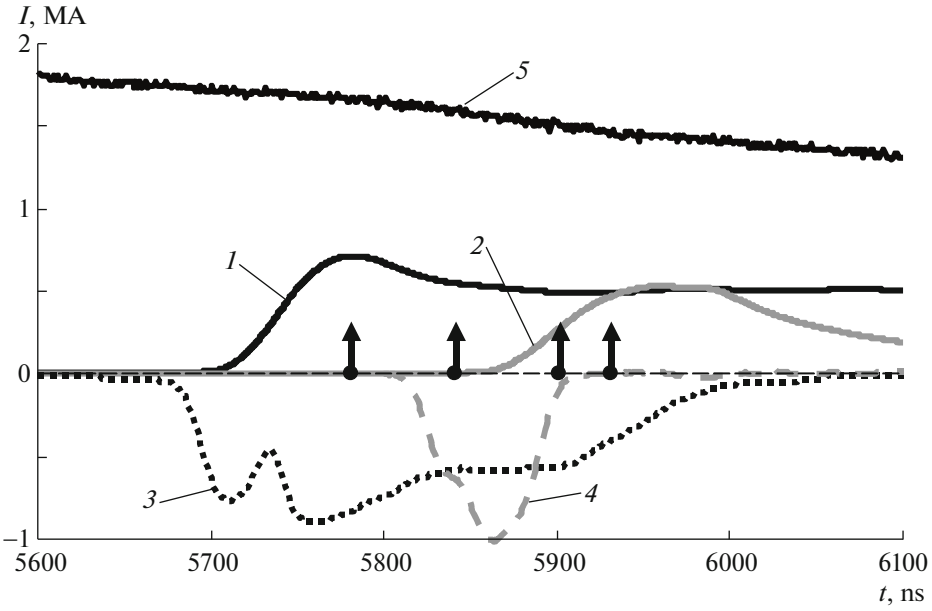

Fig. 9. The results of measuring the magnetic fields on the PF-1000 facility using a magnetic probe with a 2.5-mm-diameter cylindrical ceramic shell (shot no. 9373). Gaseous D_2, $P_0 = 1.2$ Torr, $U_0 = 24$ kV, $W_0 = 384$ kJ, $Y_n = 3.2 \times 10^{10}$ neutrons/pulse: (*1*, *2*) currents that were measured with probes positioned at radii of 40 and 13 mm, respectively; (*3*, *4*) optical signals (in arb. units) that were recorded with the probes at the same radii, respectively; and (*5*) the total discharge current; arrows mark the times of frames of laser interferometry that are shown in Fig. 10.

beams: the probe recorded similar and bipolar signals within a period of time that exceeded the implosion time T_{imp} of plasma of the multiwire array (see Fig. 6a). The time T_{imp} was determined as the time interval between the current-pulse onset ($t = 0$) and the time of the X-ray power pulse maximum (P_{SXR}). In this case, the probe with a cylindrical shell registers a signal that is approximately 12 times smaller than that registered by a probe with a flat shell in the form of a plate; the latter design is shown in Fig. 5b. If the diameter of the cylindrical shell decreases from 3 to 1.2 mm, the ratio of the recorded signals from such a probe and a flat probe is reduced to 2–6 (see Fig. 7b).

A test experiment with a probe without a protective shield was also performed in order to reveal the influence of this shield on the level of the registered magnetic field. In this case, the probe loops (their diameter was 300 μm) were immersed directly in plasma. The serviceability time of this probe was ~25 ns (see Fig. 7a), which is much shorter than the wire-array implosion time T_{imp}. In this case, the probe without a protective shell and the probe with a flat protective shell register signals with similar amplitudes and shapes within the specified period of time. Hence, an important conclusion follows that the flat shape of the probe shell does not affect the level of the probe-registered signal.

It was shown experimentally and theoretically in [4, 5] that to correctly register the magnetic field, it is important to select the size of the probe shell such that it would be thinner than the skin layer for the magnetic field in plasma and its shape would have a small cross section in the incident plasma flow (flat shell). Subsequently, miniature probes with flat shells were used in all experiments. The design of the probe with the flat shape of the protective shell is shown in Figs. 5b–5e.

Figure 6 presents the results of experiments on verifying the performance of probes with flat shells of different designs. It is seen that a probe with a flat shell (mica + NbTi) is influenced by the electron beam (see Fig. 6a). Figure 6b shows the results of experiments with a magnetic probe with the design of the protective shell (epoxy resin + NbTi) that is shown in Fig. 5c. In this experiment, two probes of this design (probes nos. 1 and 2) and one probe (no. 3) with the (mica + NbTi, Fig. 5b) shell design were located at the same radius (8.5 mm) inside the wire array.

As follows from the results of the test, the time of a correct measurement of the magnetic field using a flat probe (epoxy resin + NbTi) is longer than the time of operation of the flat probe (mica + NbTi). One of the probes (no. 1, epoxy resin + NbTi) recorded signals for ~100 ns after the SXR pulse, while probe no. 2 of the same design ceased to correctly operate near the maximum of the P_{SXR} pulse. It should be pointed out that the correct operation of probe no. 3 stops at the instant of time that is close to the instant of generation of an electron beam with the energy $E_e < 200$ keV, while probes nos. 1 and 2 continue the correct magnetic-field measurements. In this case, slight "traces" from

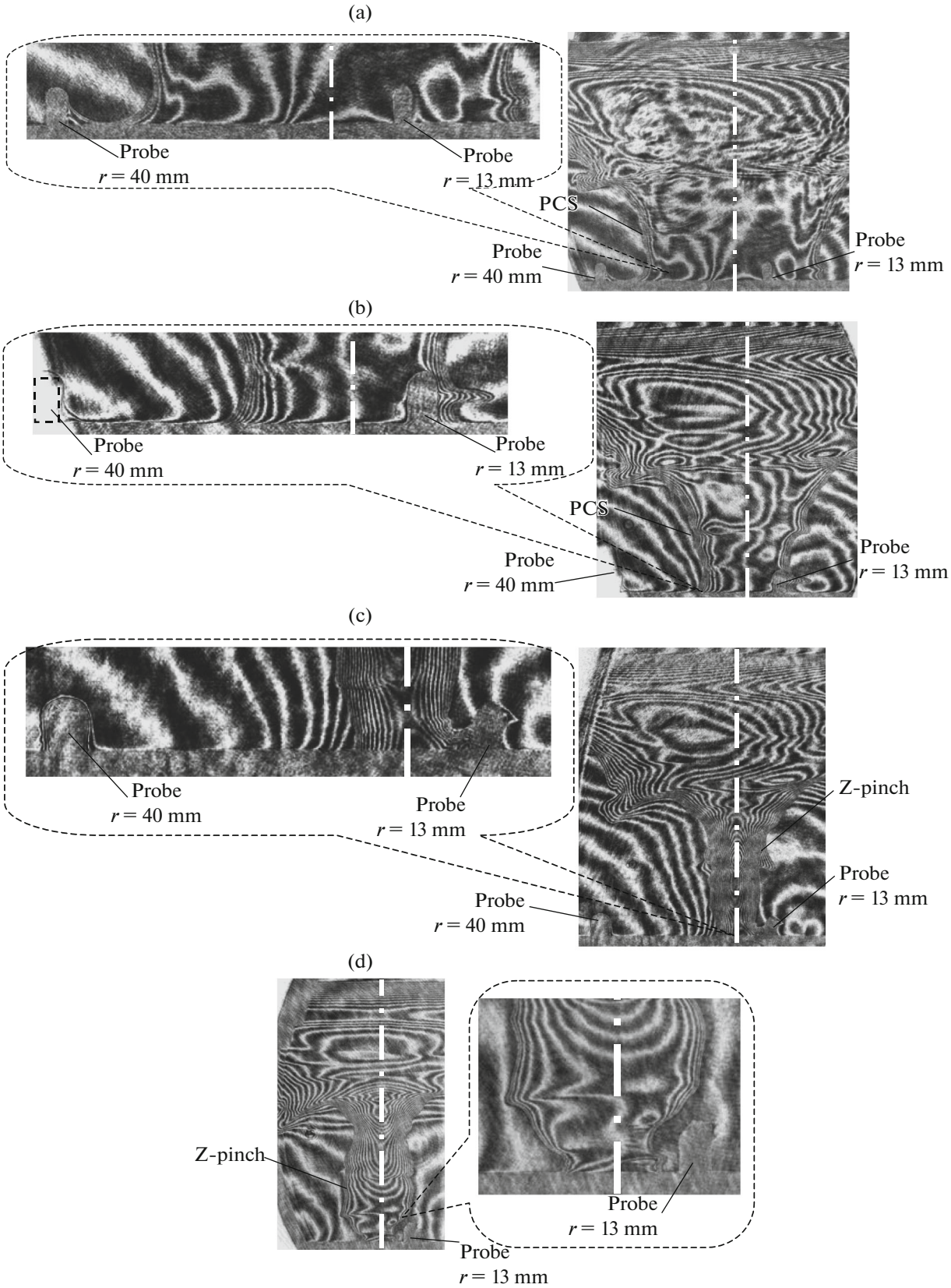

Fig. 10. The interferograms in the paraxial region at different instants of time (shot no. 9373): (a) at the 5781th ns, (b) 5841th ns, (c) 5901th ns, and (d) 5931th ns. Plasma flow around the probe with a 2.5-mm-diameter cylindrical ceramic shell. Gaseous D_2, $P_0 = 1.2$ Torr, $U_0 = 24$ kV, $W_0 = 384$ kJ, $Y_n = 3.2 \times 10^{10}$ neutrons/pulse.

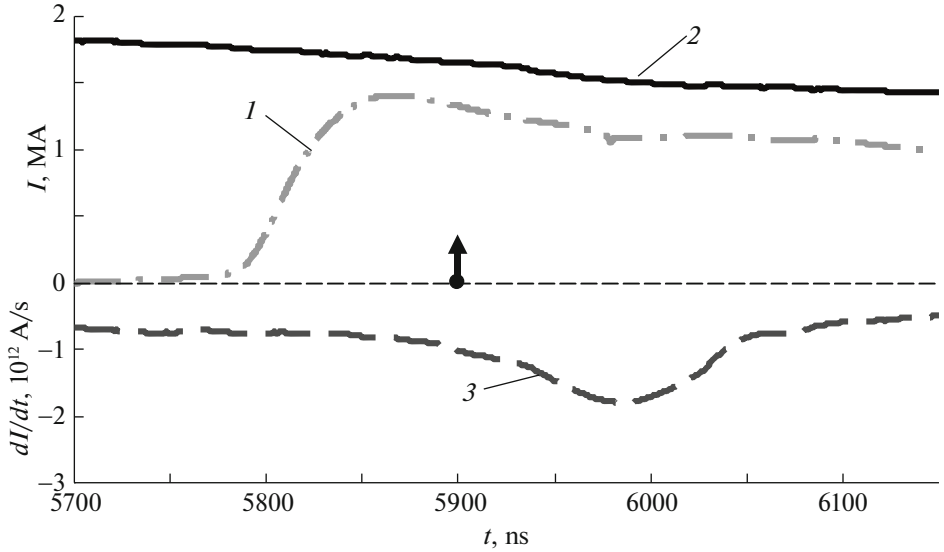

Fig. 11. The results of measuring the magnetic fields on the PF-1000 facility using a magnetic probe with a flat mica shell coated with a 15–20-μm-thick NbTi foil (shot no. 9337). Gaseous D_2, P_0 = 1.3 Torr, U_0 = 24 kV, W_0 = 384 kJ, $Y_n = 3.3 \times 10^{10}$ neutrons/pulse: (*1*) current that was measured with the probe located at a radius of 40 mm; (*2*, *3*) total discharge current and its derivative, respectively; an arrow indicates the time of the laser-interferometry frame shown in Fig. 12.

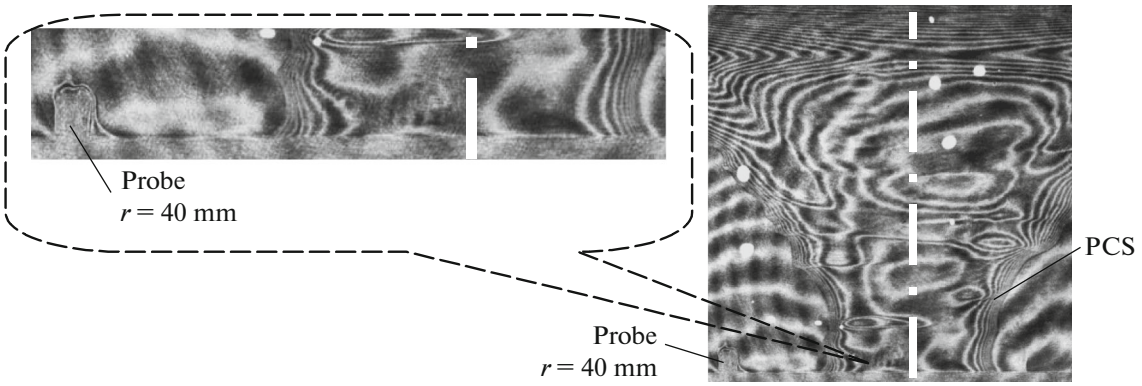

Fig. 12. An interferogram of the PCS in the paraxial region at the 5900th ns (shot no. 9337) of the discharge. Plasma flow around the probe with a flat mica shell coated with a 15–20-μm-thick NbTi foil. Gaseous D_2, P_0 = 1.3 Torr, U_0 = 24 kV, W_0 = 384 kJ, $Y_n = 3.3 \times 10^{10}$ neutrons/pulse.

the *e*-beam are observed in signals from probes nos. 1 and 2. A possible cause of the termination of the correct operation of probe no. 2 near the SXR pulse maximum (P_{SXR}) is an impact of the *e*-beam with the energy $E_e > 200$ keV on the probe.

Other designs of multilayer shells of probes were tested in comparison to a flat probe of conventional design (mica + NbTi). As can be seen in Figs. 6c, 6d, 7c, and 7d, magnetic probes with the (epoxy resin + Bi, mica + Teflon + NbTi, or W foil of thickness 20 μm) shell design record signals for a longer time (on average by 30–40 ns) than the probe with the (mica + NbTi) structure of the shell. Signals from the probes with the (epoxy resin + NbTi) design of the protective shell are affected by the electron beam to a lower degree (see Fig. 6b). The probes in which additional insulation in the form of a 20-μm-thick Teflon film was used on the average continued to correctly register a signal until the SXR pulse maximum.

Thus, it was experimentally shown that probes with multilayer shells are less susceptible to an electron beam than probes with an ordinary design of the protective shell (mica + NbTi). The reliable registration of the magnetic field by probes continued until the time of the SXR pulse maximum.

It was shown experimentally that a flat shell (in the form of a thin plate), which is oriented along the incoming plasma stream, should be preferred rather

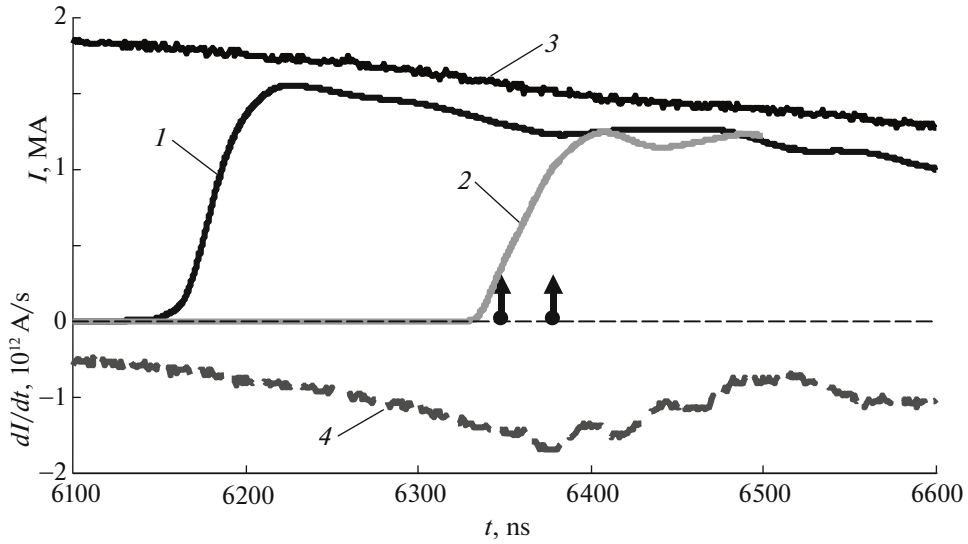

Fig. 13. The results of measuring the magnetic fields on the PF-1000 facility using a magnetic probe with a flat mica shell coated with a 15–20-μm-thick NbTi foil (shot no. 9362). Gaseous D_2, $P_0 = 1.8$ Torr, $U_0 = 24$ kV, $W_0 = 384$ kJ, $Y_n = 8.6 \times 10^{10}$ neutrons/pulse: (*1*, *2*) current that were measured with probes positioned at radii of 40 and 13 mm; (*3*, *4*) total discharge current and its derivative, respectively; arrows indicate the times of the laser-interferometry frames shown in Fig. 14.

than a cylindrical probe shell. Although reducing the diameter of a cylindrical probe shell slightly improves the situation for the reliable registration of the signal amplitude, the amplitude of the recorded signal is still several times lower than the signal amplitude from a flat probe. This is most likely related to the process of a supersonic flow of plasma with a frozen-in magnetic field around the probe shell. In this case, a flat shape of the probe shell should be preferred.

We tested the influence of the probe shape on the perturbation of investigated plasma in experiments on the PCS compression on PF facilities. The results of this test are presented below.

4. PLASMA PERTURBATION DURING ITS FLOW AROUND PROBES OF VARIOUS SHAPES

This section presents the results of studies of probe-introduced perturbations during the shrinking PCS flow around the probe in experiments on PF facilities [24–26]. The experiments were performed on two facilities with different discharge-system types: PF-3 (Filippov type, a maximum stored energy of 2.8 MJ, a current of up to 3 MA [16]) and PF-1000 (Mather type, 1 MJ, a current of up to 2 MA [27]). The degree of disturbance of the PCS plasma that is introduced by probes with cylindrical and flat shells was evaluated by means of laser interferometry in the paraxial discharge region on the PF-1000 apparatus [28].

Figure 8 shows the results of magnetic-field measurements with a cylindrical probe (curve *4*) and a probe with a flat shell (curve *2*) during the PCS compression in two shots on the PF-1000 apparatus. The probes were positioned at a distance of 40 mm from the apparatus axis. Note that for optimally selected initial conditions, the shot-to-shot repeatability was high. As an example, the total currents differed by less than 10% (curves *1* and *3*). The initial conditions for these shots were the same (gaseous D_2, $P_0 = 1.8$ Torr, $U_0 = 24$ kV, $W_0 = 384$ kJ); in this case, the integral neutron yields Y_n differed slightly: 6.9×10^{10} and 9.8×10^{10} neutrons/pulse, respectively.

As follows from Fig. 8 (curves *2* and *4*), the flat probe registers a current amplitude that exceeds that of the cylindrical probe by a factor of 1.6. The signal fronts are similar. 150 ns after the maximum, the signals from the probes coincide for 200 ns. The further divergence of signals occurs after the plasma compression and may be associated with different scenarios of the development of pinch-current shunting for these shots both near the axis of the apparatus and in the region of the insulator of the apparatus. The ratio of amplitudes of the currents measured by these probes was approximately 1.8 for the considered set of shots. This is confirmed by the experimental data from testing of cylindrical and flat probes that was performed on the Angara-5-1 apparatus; these data are presented above in Section 3 (Figs. 6 and 7).

The signal amplitude from the cylindrical probe is underestimated because of the larger perturbation that occurs during the plasma flow around the probe shell, as compared with the perturbation observed for the flat probe. The further coincidence of the signals (in both amplitude and shape) indicates a decay of the probe-induced perturbation in plasma. As the probe

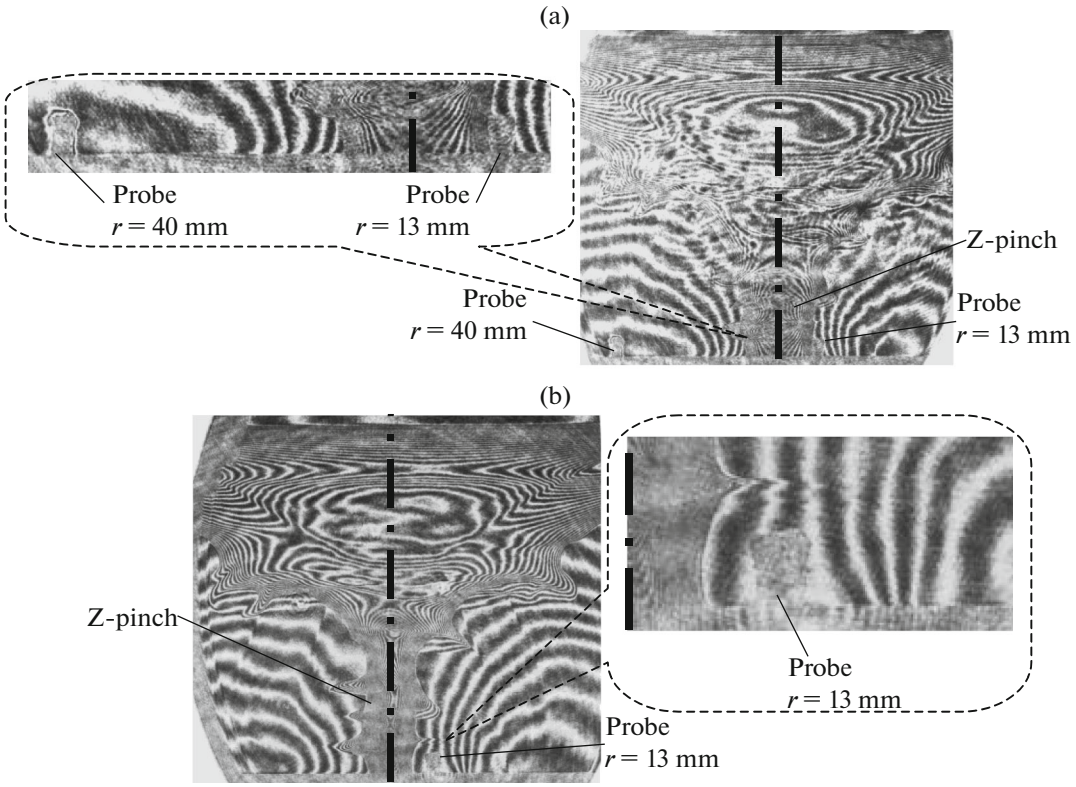

Fig. 14. Interferograms of the PCS in the paraxial region at different instants of time (shot no. 9362): at the (a) 6348th ns and (b) 6378th ns. Plasma flow around the probe with a flat mica shell coated with a 15–20-μm-thick NbTi foil. Gaseous D_2, $P_0 = 1.8$ Torr, $U_0 = 24$ kV, $W_0 = 384$ kJ, and $Y_n = 8.6 \times 10^{10}$ neutrons/pulse.

size decreases or its cross section in the incoming plasma stream becomes smaller, the plasma perturbation decreases as well and decays more rapidly with time. This is also qualitatively confirmed by the results of laser interferometry.

The results of studies of the plasma flow around the cylindrical probe (a 2.5-mm-diameter ceramic tube) by means of laser interferometry are presented below. Figure 9 shows the results of measuring the magnetic fields (currents) by cylindrical magneto-optical probes, which are positioned at different radii of 40 and 13 mm. The design of this probe is described in detail in [17, 29]. Along with a magnetic signal (curves *1* and *2*), this probe registers the optical glow of the plasma sheath (curves *3* and *4*) using an optical fiber that is mounted inside it.

The simultaneous recording of magnetic and optical signals allows investigation of the fine PCS structure: shock wave–magnetic piston. An optical signal begins to be registered earlier than a magnetic signal from the loops of the probe, thus indicating that the PCS consists of a shock wave that propagates at the head and heats and ionizes the raked gas in the magnetic-piston region, where a larger part of the plasma-sheath current flows. As was already shown, the currents that are measured with cylindrical probes are underestimated by a factor of approximately 1.6–1.8 in comparison with measurements using flat probes.

It should be noted that the probe-measured current in plasma not only greatly differs from the total current (it is approximately 2 times smaller), but it also does not correspond to the neutron yield $Y_n = 3.2 \times 10^{10}$ neutrons/pulse that was obtained in this shot. Therefore, in this case, it is incorrect to measure the dependence of the neutron yield on the current that flows in the pinch plasma. As can be seen from Fig. 10a, the scale of the plasma perturbation by the cylindrical probe at a radius of 40 mm is 2–3 sizes of the probe. Something like a "trail" stretching along the radius from the PCS to the probe (see the magnified fragment in the same figure) is observed. The PCS has not yet reached the probe at a radius of 13 mm; therefore, the latter does not register a signal, neither optical nor magnetic one. In 60 ns, the plasma perturbation that is introduced by the probe at a radius of 40 mm is greatly reduced (Fig. 10b) and almost completely vanishes 60 ns later (Fig. 10c). At the same time, plasma starts to flow around the other probe at a radius of 13 mm. By the time of the final plasma compression on the axis of the apparatus (see Fig. 10d), the plasma perturbation from the probe at a radius of 13 mm is also greatly reduced.

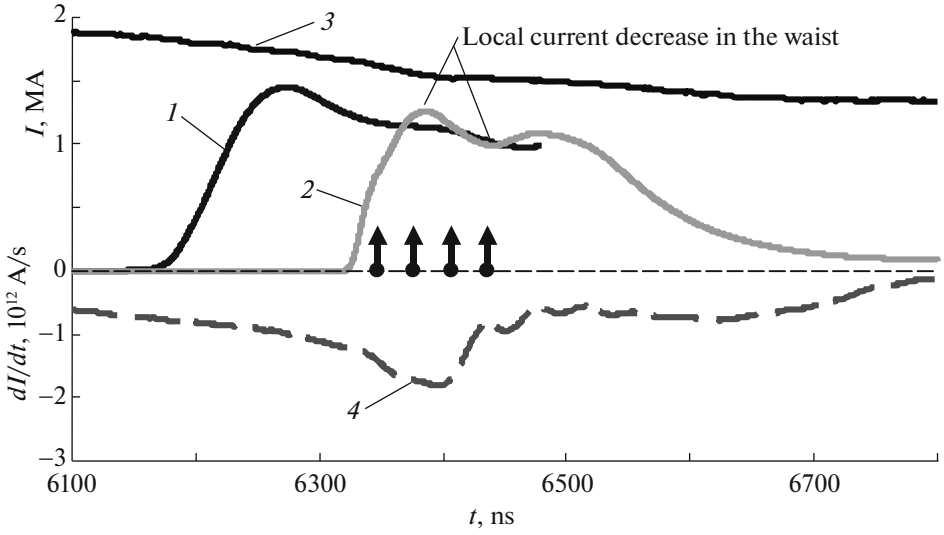

Fig. 15. The results of measuring the magnetic fields on the PF-1000 facility using a magnetic probe with a flat mica shell coated with a 15–20-μm-thick NbTi foil (shot no. 9364). Gaseous D_2, $P_0 = 1.8$ Torr, $U_0 = 24$ kV, $W_0 = 384$ kJ, $Y_n = 4.5 \times 10^{10}$ neutrons/pulse: (*1*, *2*) currents that were measured with probes positioned at radii of 40 and 13 mm; (*3*, *4*) total discharge current and its derivative, respectively; arrows indicate the times of the laser-interferometry frames shown in Fig. 16.

Figures 11–16 present the data that were obtained in experiments with a flat probe. Probes with flat shells were situated on the same radii (40 and 13 mm) as the cylindrical probes. It should be noted that the amplitude values of the currents that were recorded with the flat probes are higher than those of the currents recorded with the cylindrical probes under similar experimental conditions. Thus, for the same neutron-yield level ($Y_n \approx 3 \times 10^{10}$ neutrons/pulse), the current amplitude measured with the flat probe (Fig. 11, curve *1*) is ~1.8 times larger than that measured with the cylindrical probe (Fig. 9, curve *1*). In this case, the level of perturbation in plasma (at most 0.5 of the probe size along the radius) that flows around the flat probe is 4–6 times lower than the plasma perturbation (2–3 probe sizes) induced by the cylindrical probe. This is observed in the interference pattern in Fig. 12.

A similar pattern is observed for the flat probe located at a radius of 13 mm (Figs. 13–16). The plasma perturbation that is introduced by the flat probe is not only less than the perturbation in the case of the cylindrical probe, but it also decays more rapidly. Figure 14b shows that immediately after the PCS passes a radius of 13 mm, a plasma perturbation in the region of the flat probe is almost not observed. At the time of the maximum plasma compression near the anode, the probe registers a local current decrease (Fig. 15, curve *2*), which is associated with a dissipation of the electromagnetic energy in the compression region, that is, a "waist" in the pinch (see Fig. 16d).

To quantitatively evaluate the probe-introduced plasma perturbation, we can analyze the interference patterns for two probes: with a cylindrical shell (Fig. 10a) and a flat shell (Fig. 12). The difference between the radial distribution of the number of fringes in the perturbed part of the interferogram and the distribution of the number of fringes in the unperturbed part shows the degree of perturbation of the plasma sheath by the probe. In the case of a probe with a cylindrical shell, the disturbance of the plasma flow is ~5–6 times stronger than in the case of a probe with a flat shell, whose dimension along the incoming plasma stream was smaller than the current skin-layer in the PCS plasma.

The experiments on recording the magnetic field in the paraxial region that were performed on the PF-1000 facility showed the importance of the correct choice of the probe-shell shape in the form of a flat plate.

Similar experiments on measuring the magnetic fields were carried out with magnetic probes of similar design on the PF-3 apparatus in discharges in various working gases: argon, neon, and deuterium [16, 17]. Unlike the experiments with the probes on the PF-1000 apparatus, the cylindrical probes on PF-3 were located at considerable distances from the axis of the apparatus. Figures 17–19 show the results of magnetic-field measurements at the stage of the PCS acceleration from the anode edge to the axis.

Probes with 2.5-mm-diameter cylindrical shells were located at far radii of 160–460 mm, while a probe with a flat shell was near the axis, at a radius of 20 mm. As was shown in the experiment, after the passage of the PCS, the cylindrical probes register a current equal to the total current at a given instant of time, thus indicating the absence of a current leakage and the efficient raking of gas by the plasma sheath. At this dis-

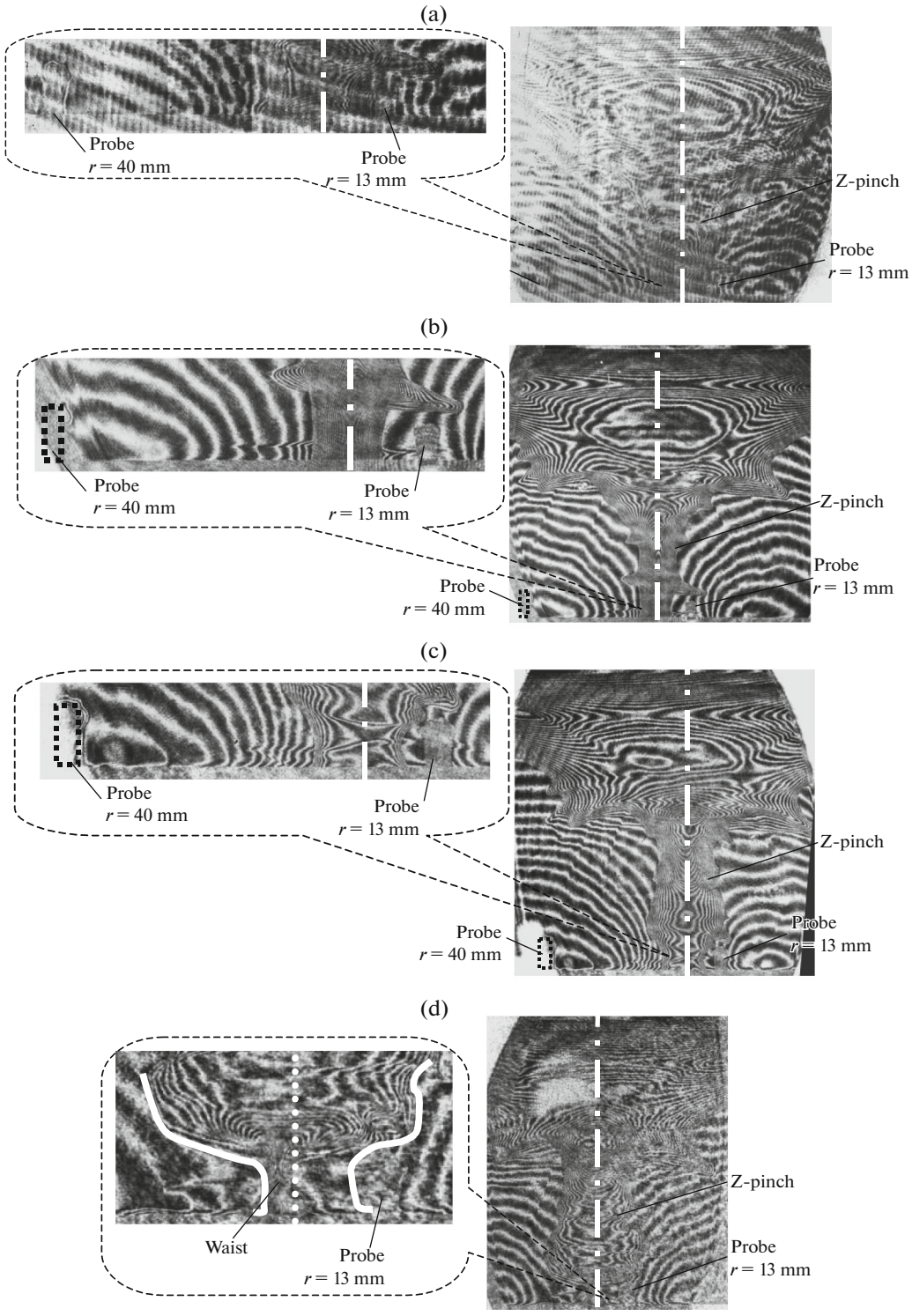

Fig. 16. Interferograms of the PCS in the paraxial region at different time (shot no. 9364): at the (a) 6347th ns, (b) 6377th ns, (c) 6407th ns, and (d) 6437th ns. Plasma flow around the probe with a flat mica shell coated with a 15–20-μm-thick NbTi foil. Gaseous D_2, $P_0 = 1.8$ Torr, $U_0 = 24$ kV, $W_0 = 384$ kJ, and $Y_n = 4.5 \times 10^{10}$ neutrons/pulse.

charge stage, the PCS has a "loose" structure: a large skin-layer thickness of 3–6 cm and a low density. In this case, the size of the cylindrical probe is less than the skin layer, thus providing a smaller plasma perturbation in the flow and a correctly recorded current by such a probe.

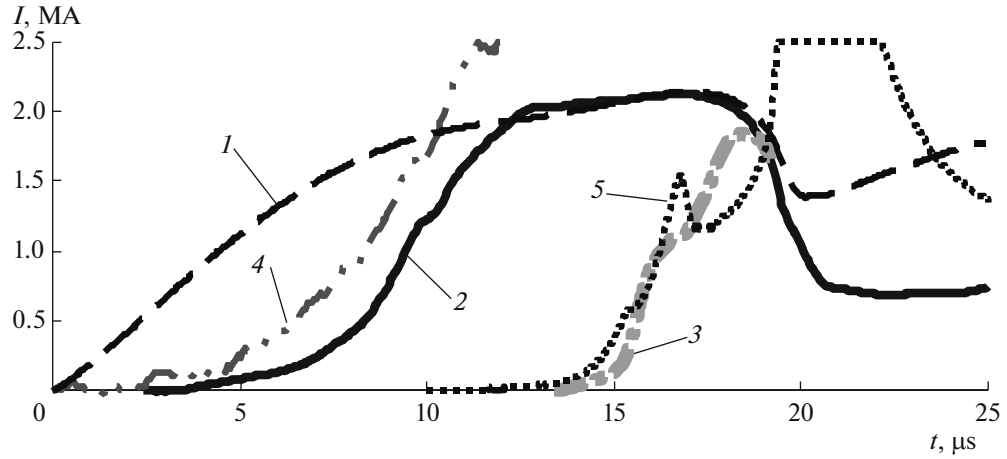

Fig. 17. The results of measuring the magnetic fields on the PF-3 facility using a magnetic probe with a 2.5-mm-diameter cylindrical ceramic shell (shot no. 4103). Gaseous D_2 + Xe(3%), P_0 = 3 Torr, U_0 = 11 kV, W_0 = 500 kJ, and $Y_n = 1.6 \times 10^{10}$ neutrons/pulse: (*1*) total discharge current; (*2*, *3*) currents that were measured with probes positioned at radii of 460 and 260 mm, respectively; (*4*, *5*) optical signals (in arb. units) that were recorded with the probes at the same radii, respectively.

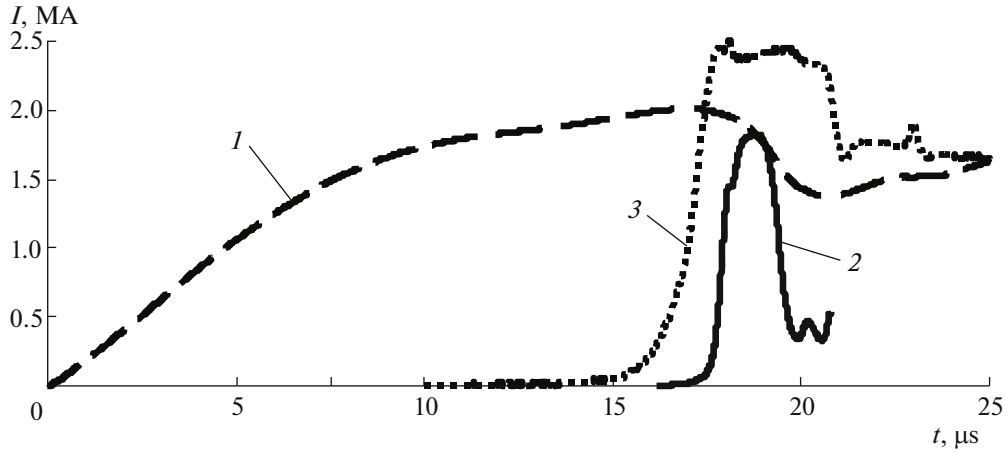

Fig. 18. The results of measuring the magnetic fields on the PF-3 facility using a magnetic probe with a 2.5-mm-diameter cylindrical ceramic shell (shot no. 4108). Gaseous D_2 + Xe(3%), P_0 = 3 Torr, U_0 = 11 kV, W_0 = 500 kJ, and $Y_n = 4.0 \times 10^9$ neutrons/pulse: (*1*) total discharge current and (*2*, *3*) current and optical signals (in arb. units) that were recorded with the probe positioned at a radius of 260 mm.

Estimates on the basis of the experimental data from [16] show that in the paraxial region of the apparatus ($r < 20$ mm), the skin-layer of the PCS is already ~1 cm; therefore, the probe size should be at least several times smaller, 1–3 mm. In this case, we used a flat probe with a thickness of ~0.5 mm and a length along the incoming plasma stream of ~2 mm. The results of current measurements (curve *6*) with such a probe are shown in Fig. 19. The amplitude of the current that was measured with the flat probe at a radius of 20 mm coincides with the amplitude that was measured using the cylindrical probe at a radius of 160 mm at the same instant of time, and the subsequent behavior of the curves of these currents is completely identical.

Experiments on the PF-3 facility have shown that the use of cylindrical probes is possible at the early stages of the PCS acceleration, when the skin effect for the magnetic field in the plasma sheath is poorly pronounced and the skin-layer thickness exceeds the probe size. In the paraxial region of the facility where the plasma sheath is compressed with a high speed ($V_r \sim 10^7$ cm/s), it is obligatory to use a flat probe.

5. SELECTING THE SHAPE AND MATERIAL OF THE PROBE SHELL

Difficulties in direct detailed measurements of plasma parameters in a plasma flow around a mag-

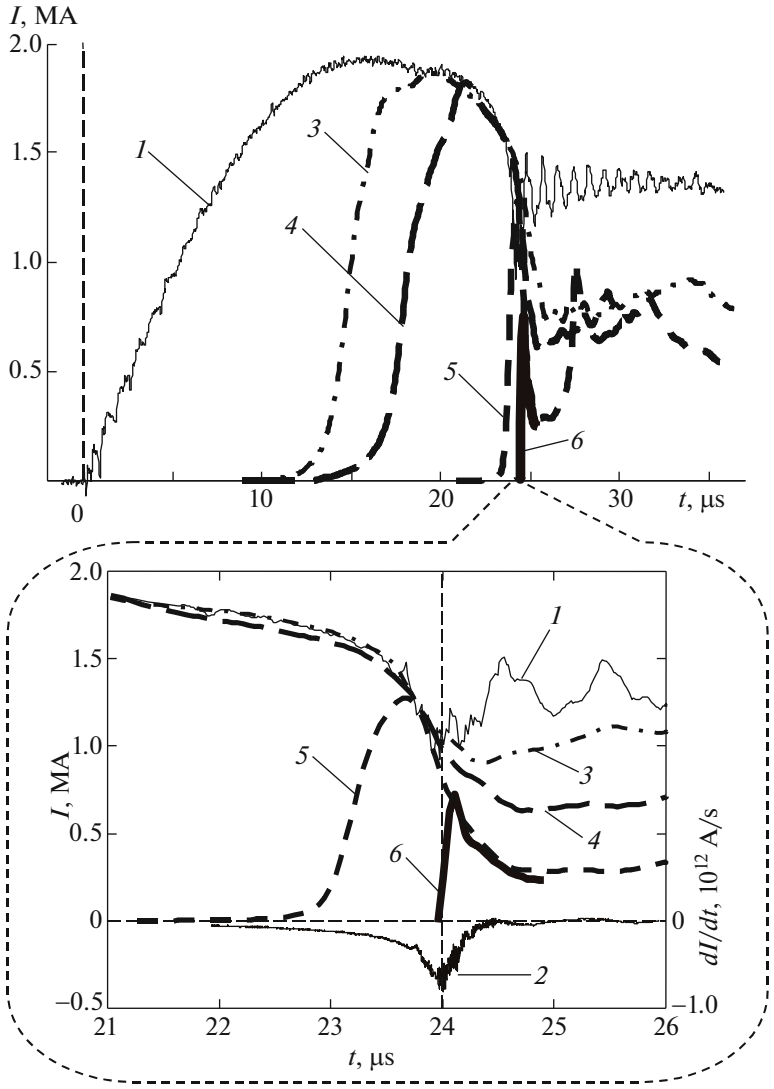

Fig. 19. The results of measuring the magnetic fields on the PF-3 facility (shots nos. 4027, 4029). Gaseous Ar, $P_0 = 1.5$ Torr, $U_0 = 8$ kV, and $W_0 = 260$ kJ: (*1*, *2*) total discharge current and its derivative; (*3*, *4*, *5*) currents that were measured with cylindrical probes positioned at radii of 460, 360, and 160 mm, respectively; and (*6*) current that was measured with a flat probe positioned at a radius of 20 mm.

netic probe and the problems of interpreting the measurement results determine the important role of numerical modeling. Processes in the radiating multiply charged plasma are diverse and interrelated. It is necessary to take the following processes into account: the motion of matter in the framework of magnetic hydrodynamics (MHD), the diffusion of the magnetic field, the thermal conductivity, the radiation transport, and the substance ionization. One should also consider the magnetization of the transport coefficients. For the numerical simulation of a magnetized-plasma flow around a body in a supersonic mode and a mode that is close to it, a 2D MHD program was used in [5], which was developed at the Russian Federal Nuclear Center–VNIITF and refined for calculating the problems of the plasma flow around bodies of various shapes (cylindrical and elliptic) in a magnetic field.

The parameters of plasma that was incident on a probe were similar to those observed on the Angara-5-1 facility and varied within the following ranges: the electron density, 5×10^{17}–1×10^{19} cm^{-3}; the plasma velocity, 1×10^6–5×10^7 cm/s; the magnetic field, 0–100 kG; the temperature, 1–30 eV; and the conductivity was assumed to be of the Spitzer type. The cylindrical and elliptic probes were compared. The latter shape of the probe shell was chosen as the most approximate shape to that of a flat probe, which was used in our experiments.

The calculations made it possible to assess the level of the probe-introduced plasma perturbation. The magnetic-field perturbation was determined as the

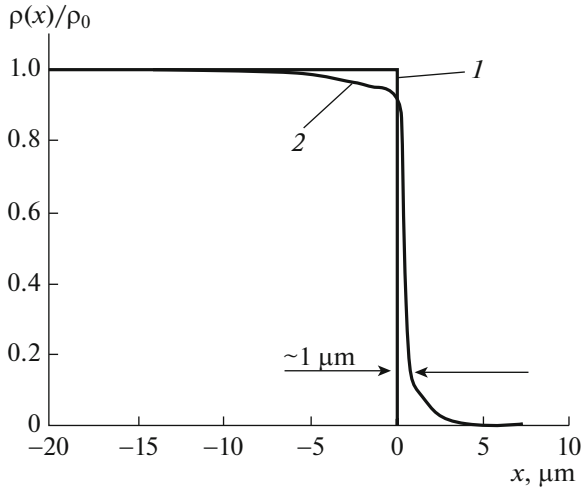

Fig. 20. The results of the numerical simulation of the evaporation of the probe's NbTi-shell edge (boundary) under the influence of X rays from plasma that flows around the probe. The calculated distribution of the probe-shell density $\rho(x)$ divided by the initial density of the shell material ρ_0: (*1*) initial distribution and (*2*) after the action of X-ray radiation.

ratio of the fields at the observation point to the unperturbed magnetic field: $B_\varphi/B_\varphi^\infty$. As was shown by calculations, the magnetic-field perturbation in plasma at the frontal point of the cylindrical shell of the probe was as high as ~60%. In the region of the measuring loops that were located inside the cylindrical shield, the magnetic field was generally lower than the undisturbed magnetic-field level by approximately 1.3–1.4 times. The plasma perturbation for a stationary plasma flow extended to 3–4 sizes of the cylindrical probe. This result qualitatively confirms the experimental results of the flow around cylindrical probes in the Angara-5-1 and PF-1000.

In contrast, the magnetic-field perturbation in plasma at the frontal point of the elliptic shell of the probe was small (~7%); in the region of the measuring loops, the perturbation was even smaller, 3–5%. The spatial extent of the plasma perturbation behind the probe was also small and amounted to no more than one probe size along the plasma motion direction.

Since the probe is in direct contact with strongly radiating plasma, the probe shell material evaporates under the influence of X rays. The intense evaporation of the probe-shell substance may cause intense radiative cooling of the diagnosed plasma. The performed calculations of a stationary supersonic plasma flow around the probe took the evaporation of the probe-shell substance into account. It was shown that when tungsten plasma with an ion concentration of $\sim 10^{18}$ particles/cm^3, a temperature of 25 eV, and an initial degree of ionization of 5 irradiates a NbTi foil for 100 ns, the probe-shell substance evaporates on a thickness of at most 1 μm (Fig. 20).

To assess the thickness of a shell of other substances (Cu, Nb, and Ti) that is ablated under the exposure to a pulse of soft X rays, the heat-conduction equation was solved. The layer of the probe-shell material where the energy per particle exceeded the sublimation energy for this substance was considered sublimated. The thickness of the ablated shell was 1.9, 1.2, and 1.1 μm for Cu, Nb, and Ti, respectively. The number of sublimated particles was 4×10^{18} (for Cu), 1.6×10^{18} (Nb), 1.5×10^{18} (Ti), and 1.0×10^{18} (NbTi). As is seen, the minimum number of ablated particles is observed when an NbTi foil is used for the probe shell. Thus, the contamination of the investigated plasma with impurities can be reduced.

It should be noted that the radiative cooling of plasma around the probe will lead to a decrease in its conductivity and, as a consequence, will somewhat improve the diffusion times of the magnetic field from plasma to the interior of the probe shield. Thus, the performed numerical modeling has shown the importance of choosing the shape and material of the probe shell.

6. CONCLUSIONS

The performed experimental check of the performance of the magnetic-probe technique for measuring the magnetic fields in plasma with a high energy release (up to 1 TW/cm^2), which is produced on high-current facilities, makes it possible to conclude:

(1) Magnetic probes with multilayer shells that protect against the exposure to electron beams with energies of up to 150 keV were designed and tested on the Angara-5-1 facilities. This made it possible to extend the time of recording the magnetic field at the stage of the final plasma compression and yield of soft X-rays. The small dimensions of the loops of the probes determine the spatial resolution of this technique as ~300 μm. The probes provide a time resolution in the nanosecond range of no worse than 1.5 ns. The absolute calibration of the effective area of the measuring loops, considering the plasma flow around the probe, and the correct choice of the probe-shell shape provide an accuracy of 20% of the magnetic-field measurements in plasma.

(2) The possibility of using a shell-less probe (open loops placed in plasma) for 20–25 ns was demonstrated for the experimental conditions on the Angara-5-1 apparatus (the current is up to 4 MA and the SXR power flux is up to 1 TW/cm^2).

(3) The use of a cylindrical probe with a size that exceeds the skin layer of the magnetic field in plasma in studies of the PCS near the axis of a PF apparatus introduces appreciable perturbations into plasma and distorts the recorded signals. For the experimental conditions on the PF-1000 apparatus, the amplitudes of signals that are registered by a cylindrical probe with a 2.5-mm diameter are underestimated by a factor of

~1.6–1.8. Conversely, the use of a magnetic probe with a flat shell introduces minimum perturbations into plasma and does not distort the probe readings.

(4) The use of a cylindrical probe with the same dimensions for the experimental conditions on the Angara-5-1 facilities showed an even larger distortion of the probe signal in both the amplitude (a 12-fold decrease) and the leading edge in comparison with a signal from the flat probe. A decrease in the diameter of the cylindrical shell from 3 to 1.5 mm results in a slightly improved situation: the underestimation of the recorded signal amplitude decreases from a factor of 12 to 2–6 at different plasma-compression stages.

(5) The experiments on the PF-3 installation demonstrated the applicability of large cylindrical probes with a 2.5-mm diameter in studies of the PCS at the stages of its formation and acceleration at long distances from the installation axis (160–460 mm). In this case, the probe size is smaller than the skin layer for the magnetic field in the still forming "loose" PCS structure (shock wave–magnetic piston). The estimate of the skin layer of the magnetic field in plasma at this discharge stage lies between 3 and 6 cm depending on the distance to the installation axis. A probe with a flat shell was successfully used at the final stage of the PF formation in the paraxial region of the installation (1–2 cm from the axis).

(6) The versatility of the design of magnetic probes makes it possible to use them in investigations of high-temperature dense plasma in generators of superhigh electric power and on PF-type facilities.

ACKNOWLEDGMENTS

We are grateful to I.V. Glazyrin and A.V. Karpeev for conducting numerical MHD calculations of the plasma flow around a magnetic-probe shell, A.Yu. Koshelev for the manufacture of magnetic probes, V.P. Vinogradov for his help in the protection of sections for recording signals from magnetic probes against electromagnetic interference, and the teams of the Angara-5-1, PF-3, and PF-1000 facilities for the engineering and technological support of the experiments.

This study was supported by the Russian Foundation for Basic Research (projects nos. 16-02-00084, 14-29-06085_OFI_M, and 17-02-01184-a).

REFERENCES

1. Bruzzone, H. and Grondona, D., *Plasma Phys. Control. Fusion*, 1997, vol. 39, no. 9, p. 1315. doi 10.1088/0741-3335/39/9/004
2. Bruzzone, H. and Martinez, J.F., *Plasma Sources Sci. Technol.*, 2001, vol. 10, no. 3, p. 471. doi 10.1088/0963-0252/10/3/312
3. Bruzzone, H., Moreno, C., and Kelly, H., *Meas. Sci. Technol.*, 1991, vol. 2, no. 12, p. 1195. doi 10.1088/0957-0233/2/12/015
4. Grabovskii, E.V., Zukakishvili, G.G., Mitrofanov, K.N., Oleinik, G.M., Samokhin, A.A., and Smirnov, V.P., *Preprint of GNC RF TRINITI*, 2002, CNIIATOM-IFORM, no. 0091A, p. 40. http://www.twirpx.com/file/843831/
5. Glazyrin, I.V., Grabovskii, E.V., Zukakishvili, G.G., Karpeev, A.V., Mitrofanov, K.N., Oleinik, G.M., and Samokhin, A.A., *Probl. Atom. Sci. Technol., Ser. Thermonucl. Fusion*, 2009, no. 2, p. 67.
6. Al'bikov, Z.A., Velikhov, E.P., Veretennikov, A.I., Glukhikh, V.A., Grabovskii, E.V., Gryaznov, G.M., Gusev, O.A., Zhemchuzhnikov, G.N., Zaitsev, V.I., Zolotovskii, O.A., Istomin, Yu.A., Kozlov, O.V., Krasheninnikov, I.S., Kurochkin, S.S., Latmanizova, G.M., et al., *At. Energ.*, 1990, vol. 68, no. 1, p. 26.
7. Kurtmulaev, R.Kh., Pilsky, V.I., and Semenov, V.N., *Zh. Tekh. Fiz.*, 1970, vol. 40, no. 5, p. 1044.
8. Bhuyan, H., Mohanty, S.R., Neog, N.K., Bujarbarua, S., and Rout, R.K., *Meas. Sci. Technol.*, 2003, vol. 14, no. 10, p. 1769. doi 10.1088/0957-0233/14/10/305
9. *Plasma Diagnostics,* Lokhte-Holtgreven, W., Ed., Kiel Univers., Amsterdam: North-Holland, 1968.
10. Mohammadi, M.A., Sobhanian, S., Ghomeishi, M., Ghareshabani, E., Moslehi-fard, M., Lee, S., and Rawat, R.S., *J. Fusion Energy*, 2009, vol. 28, no. 4, p. 371. doi 10.1007/s10894-009-9205-2
11. Zakaullah, M., Ahmad, Imtiaz., Murtaza, G., and Beg, M.M., *Fusion Eng. Des.,* 1997, vol. 36, no. 4, p. 437. doi 10.1016/S0920-3796(97)00072-0
12. Gurey, A., Nikulin, V., Polukhin, S., and Volobuev, I., *Probl. Atom. Sci. Technol.(PAST), Ser. Plasma Phys.,* 2009, vol. 15, no. 1, p. 98.
13. Bakhtin, V.P., Skvortsov, Yu.V., and Umrikhin, N.M., *Plasma Dev. Oper.,* 1992, vol. 2, no. 2, p. 141. doi 10.1080/10519999208240676
14. Krauz, V.I., Mitrofanov, K.N., Myalton, V.V., Khautiev, E.Yu., Mokeev, A.N., Vinogradov, V.P., Vinogradova, Yu.V., Grabovsky, E.V., and Zukakishvili, G.G., http://epsppd.epfl.ch/Warsaw/pdf/P1_018.pdf
15. Krauz, V.I., Mitrofanov, K.N., Myalton, V.V., Grabovski, E.V., Koidan, V.S., Vinogradov, V.P., Vinogradova, Yu.V., and Zukakishvili, G.G., *IEEE Trans. on Plasma Sci.*, 2010, vol. 38, no. 2, p. 92. doi 10.1109/TPS.2009.200036916
16. Krauz, V.I., Mitrofanov, K.N., Myalton, V.V., Vinogradov, V.P., Vinogradova, Yu.V., Grabovskii, E.V., Zukakishvili, G.G., Koidan, V.S., and Mokeev, A.N., *Plasma Phys. Rep.,* 2010, vol. 36, no. 11, p. 937. doi 10.1134/S1063780X10110036
17. Krauz, V.I., Mitrofanov, K.N., Myalton, V.V., Vinogradov, V.P., Vinogradova, Yu.V., Grabovskii, E.V., and Koidan, V.S., *Plasma Phys. Rep.,* 2011, vol. 37, no. 9, p. 742. doi 10.1134/S1063780X11080058
18. Krauz, V., Mitrofanov, K., Scholz, M., Paduch, M., Karpinski, L., Zielinska, E., and Kubes, P., *Plasma Phys. Contr. Fusion,* 2012, vol. 54, no. 2, p. 025010. doi 10.1088/0741-3335/54/2/025010
19. Gribov, A.N., Aleksandrov, V.V., Grabovskiy, E.V., Gritsuk, A.N., Medovshikov, S.F., Mitrofanov, K.N., and Oleinik, G.M., *IEEE Trans. on Plasma Sci.*, 2009, vol. 37, no. 10, part 1, p. 1981. doi 10.1109/TPS.2009.2018554

20. Aleksandrov, V.V., Grabovskii, E.V., Mitrofanov, K.N., Oleinik, G.M., Smirnov, V.P., Sasorov, P.V., and Frolov, I.N., *Plasma Phys. Rep.,* 2004, vol. 30, no. 7, p. 615. doi 10.1134/1.1778432

21. Alexandrov, V.V., Fortov, V.E., Frolov, I.N., Grabovskii, E.V., Krasuk, I.K., Lomonosov, I.V., Mitrofanov, K.N., Pashinin, P.P., Semenov, A.Yu., Smirnov, V.P., Oleinik, G.M., Porofeev, I.Yu., Vovchenko, V.I., and Zukakishvili, G.G., *Proc. 13th Int. Conf. on High-Power Particle Beams* (BEAMS 2000), Nagaoka Univ. of Technol., Japan, 2000, vol. 1, p. 142.

22. Aleksandrov, V.V., Grabovski, E.V., Gribov, A.N., Gritsuk, A.N., Medovshchikov, S.F., Mitrofanov, K.N., and Oleinik, G.M., *Plasma Phys. Rep.,* 2009, vol. 35, no. 2, p. 161.

23. *Fizicheskie velichiny: Spravochnik* (Physical Quantities: a Handbook), Grigor'ev, I.S. and Meilikhov, E.Z., Eds., Moscow: Energoatomizdat, 1991.

24. Petrov, D.P., Filippov, N.V., Filippova, T.I., and Khrabrov, V.A., *Fizika plazmy i problemy upravlyaemykh termoyadernykh reaktsii (Plasma Physics and Problems of Controlled Fusion Reactions),* Leontovich, M.A., Ed., Moscow: AN SSSR, 1958, vol. 4, p. 170.

25. Filippov, N.V., Filippova, T.I., and Vinogradov, V.P., *Nucl. Fusion Suppl.*, 1962, part 2, p. 577.

26. Mather, J.W., *Phys. Fluids,* 1965, vol. 8, p. 366. doi 10.1063/1.1761231

27. Scholz, M., Karpinski, L., Krauz, V.I., Kubes, P., Paduch, M., and Sadowski, M.J., *Nukleonika*, 2012, vol. 57, no. 2, p. 183.

28. Zielinska, E., Paduch, M., and Scholz, M., *Contrib. Plasma Phys.,* 2011, vol. 51, nos. 2–3, p. 279. doi 101002 /ctpp.201000047

29. Mitrofanov, K.N., Krauz, V.I., Kubesh, P., Scholz, M., Padukh, M., and Zelinska, E., *Plasma Phys. Rep.,* 2014, vol. 40, no. 8, p. 623. doi 10.1134/S1063780X14070071

Translated by A. Seferov